Available online at www.sciencedirect.com
SCIENCE @ DIRECT®

Spectrochimica Acta Part A 60 (2004) 1141–1159

SPECTROCHIMICA
ACTA
PART A

www.elsevier.com/locate/saa

Synthesis, Fourier transform infrared and Raman spectra, assignments and analysis of *N*-(phenyl)- and *N*-(chloro substituted phenyl)-2,2-dichloroacetamides

V. Arjunan[a], S. Mohan[b,*], S. Subramanian[c], B. Thimme Gowda[d]

[a] *Department of Chemistry, Tagore Arts College, Pondicherry 605008, India*
[b] *Department of Materials Science, Asian Institute of Medicine, Science and Technology, Amanjaya, 08000 Sungai Petani, Kedah Darul Aman, Malaysia*
[c] *Department of Chemistry, Pondicherry Engineering College, Pondicherry 605014, India*
[d] *Department of Chemistry, Mangalore University, Mangalore, India*

Received 3 June 2003; accepted 1 July 2003

Abstract

N-(phenyl)-2,2-dichloroacetamide (NPA) and *N*-(chloro substituted phenyl)-2,2-dichloroacetamides of the configuration $X_yC_6H_{5-y}$–NHCO–$CHCl_2$ (where, $X = Cl$ and $y = 1$, 2 and 3) were synthesised and the Fourier transform infrared (FTIR) and Fourier transform Raman (FT-Raman) spectra of the compounds were recorded and analysed. The FTIR spectra of all the compounds were recorded in a Bruker IFS 66V spectrometer in the range of 4000–400 cm^{-1} and the FT-Raman spectra were also recorded in the same instrument in the region 3500–100 cm^{-1}. The variation of an amide bond (–NHCO–) parameters with the substitution of the chlorine atom in the phenyl group and the mixing of different normal modes are discussed with the help of potential energy distribution (PED) calculated through normal co-ordinate analysis.

Keywords: FTIR; FT-Raman; Normal co-ordinate analysis; *N*-(Phenyl)-2,2-dichloroacetamides

1. Introduction

N-Phenyl acetamide (acetanilide) is an interesting system because the nearly planar amide groups display bond distances, which are close to those found in polypeptides. Since the physical properties of hydrogen bonded amide systems are very sensitive to bond distances, *N*-phenyl acetamide and its derivatives to be useful model system in the search for new physical features of extended polypeptides and perhaps even natural proteins [1–6]. Spectroscopic and crystal structural studies give valuable information on bond properties. Amides are of fundamental chemical interest as conjugation between nitrogen lone pair electrons and the carbonyl π-bond results in distinct physical and chemical properties. The amide moiety is an important constituent of many biologically significant compounds.

Many acetanilides exhibit fungicidal, herbicidal and pharmacological activities which has further stimulated recent interest in their chemistry. *N*-Phenyl acetamide is used in medicine under the name antifebrin, as a febrifuge. It is a useful intermediate in various reactions of aniline in which it is desirable to protect the amino group. The acetamido ($-NHCOCH_3$) group is predominantly *p*-orienting. Anilide herbicides are promising weed control agents for a wide variety of economically important crops including rice, cotton, potatoes and corns. The choloroacetanilde herbicide alachlor is one of the most extensively used of all the agro chemicals [7]. Among the attractive features of these herbicides are their effectiveness, selectivity and low mammalian toxicity [8,9]. Propanil (3,4-dichloropropioanilide) is a selective contact anilide herbicide recommended for post-emergence use in rice. It is commonly used for the control of broad levelled and grass weeds and is the only active substance in the phyto-pharmaceutical products.

Single crystal Raman, far infrared and inelastic neutron scattering (INS) spectra of acetanilide in the low frequency

---

* Corresponding author.
E-mail address: s_mohan@lycos.com (S. Mohan).

1386-1425/$ – see front matter © 2003 Elsevier B.V. All rights reserved.
doi:10.1016/j.saa.2003.07.003

(phonon) region were reported [10,11]. The temperature dependence infrared and Raman spectra of *N*-methylacetamide [12], acetanilide and deuterated acetanilide [13–15] were analysed. The vibrational spectra and normal vibrations of trichloroacetamide have been investigated by Sree Ramulu and Ramana Rao [16]. Vibrational spectra of some halogen substituted acetamides have been analysed by Krishnamoorthy and Ramana Rao [17–20]. The spectral investigation of tertiary amides and related systems has been reported [21,22]. The Raman and infrared spectra of *N*,*N*-diethyl formamide, *N*,*N*-diethyl acetamide and *N*,*N*-diethyl chloroacetamide were analysed by Sudarshan et al. [23]. The IR and Raman spectra of *N*-(substituted phenyl)-2,2,2-trichloroacetamides have been analysed [24]. Laser Raman and Fourier transform infrared (FTIR) spectra of *p*-nitroacetanilide were recorded and the observed bands are assigned assuming the molecules belong to the C_S point group [25]. FT-NIR spectra of *N*-methylacetamide [26] and the infrared study of dimethylacetamide [27] have been carried out. New investigations of the temperature dependence of the far-infrared spectra of acetanilide and its isotopomers have been presented by Spire et al. [28].

Studies of intermolecular associations, dichroic absorption, band contour of the vapour spectra, measurements of integrated intensities of the absorption bands and normal co-ordinate analysis give information regarding the nature of the functional groups, orbital interactions and mixing of skeletal frequencies. A systematic study on the vibrational spectra of simple primary, secondary and tertiary amides received considerable attention in the spectroscopic literature in view of their obvious importance to biological systems.

Despite the wide use of the *N*-phenyl acetamide family of molecules in various applications, their spectroscopic properties are not received much attention. Therefore, we are interested in the spectroscopic studies of amides and their derivatives. The main purpose of the present investigation is to synthesis some substituted *N*-(phenyl)-2,2-dichloroacetamides (NPA), to record the FTIR and Fourier transform Raman (FT-Raman) spectra, to assign the various fundamental modes precisely, to analyse the fundamental vibrations completely, to show how the amide bond (–NHCO–) parameters vary with the substitution of the chlorine atom in the phenyl group and to analyse the mixing of different normal modes with the help of potential energy distribution (PED) calculated through normal co-ordinate analysis. Thus, in the present investigation, we have undertaken an extensive experimental and theoretical investigation of *N*-(phenyl)-2,2-dichloroacetamide and *N*-(chloro substituted phenyl)-2,2-dichloroacetamides by recording their FTIR and FT-Raman spectra and subjecting them to normal co-ordinate analysis, in an effort to provide a possible explanations for our observations.

2. Experimental

N-(Phenyl)-2,2-dichloroacetamide and *N*-(chloro substituted phenyl)-2,2-dichloroacetamides of the configuration $X_yC_6H_{5-y}$–NHCO–$CHCl_2$ (where, X = Cl and $y = 1$, 2 and 3) were synthesised from the respective chloroanilines, dichloroacetic acid and phosphorusoxychloride [24,29]. The pure samples of aniline, respective chloroanilines, dichloroacetic acid and phosphorus oxychloride were purchased from Aldrich, USA with stated purity and are used as such without further purification. All other chemicals employed are of AR grade. Dichloroacetic acid and phosphorus oxychloride were mixed together slowly to obtain a clear mixture. To this aniline/respective chloroanilines has been added with constant stirring. The mixture was slowly warmed to expel the hydrochloric acid formed. Cold water was added to hydrolyse the excess phosphorus oxychloride present. The hydrochloric acid produced was removed by treating with excess of 2N sodium hydroxide solution, there by the crude products were formed, separated, washed with water and dried. The crude samples were recrystallised from ethanol. The melting points of the recrystallised samples were determined. The purity of the compounds was confirmed by chemical analysis for C, H and N. The FTIR spectra of all the compounds were recorded in a Bruker IFS 66V spectrometer in the range of 4000–400 cm^{-1}. The spectral resolution was ±2 cm^{-1}. The FT-Raman spectra of these compounds were also recorded in the region 3500–100 cm^{-1} using the same instrument with FRA 106 Raman module equipped with Nd:YAG laser source operating at 1.064 μm line with 200 mW power of spectral width 2 cm^{-1}. The frequencies of all sharp bands are accurate to ±1 cm^{-1}. The melting point (m.p.) and the elemental analysis of the compounds are presented in Table 1.

Table 1
Melting points and elemental analysis of the compounds studied

S. No.	Name of the compound	Melting point (°C)	Found (calculated) (%)		
			C	H	N
1	*N*-Phenyl-2,2-dichloroacetamide	109	47.01 (47.07)	3.42 (3.46)	6.81 (6.87)
2	*N*-(2-Chlorophenyl)-2,2-dichloroacetamide	103	40.19 (40.27)	2.49 (2.54)	5.82 (5.87)
3	*N*-(4-Chlorophenyl)-2,2-dichloroacetamide	127	40.22 (40.27)	2.50 (2.54)	5.81 (5.87)
4	*N*-(2,3-Dichlorophenyl)-2,2-dichloroacetamide	136	35.01 (35.18)	1.79 (1.85)	5.03 (5.13)
5	*N*-(2,4-Dichlorophenyl)-2,2-dichloroacetamide	131	35.04 (35.18)	1.80 (1.85)	5.09 (5.13)
6	*N*-(2,3,4-Trichlorophenyl)-2,2-dichloroacetamide	88	31.11 (31.24)	1.26 (1.31)	4.50 (4.56)
7	*N*-(2,4,6-Trichlorophenyl)-2,2-dichloroacetamide	187	31.15 (31.24)	1.28 (1.31)	4.99 (4.56)

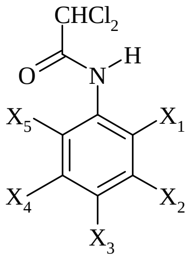

(i) NPA : $X_1, X_2, X_3, X_4, X_5 = H$
(ii) 2CPA : $X_1 = Cl$ and $X_2, X_3, X_4, X_5 = H$
(iii) 4CPA : $X_3 = Cl$ and $X_1, X_2, X_4, X_5 = H$
(iv) 23CPA : $X_1, X_2 = Cl$ and $X_3, X_4, X_5 = H$
(v) 24CPA : $X_1, X_3 = Cl$ and $X_2, X_4, X_5 = H$
(vi) 234CPA : $X_1, X_2, X_3 = Cl$ and $X_4, X_5 = H$
(vii) 246CPA : $X_1, X_3, X_5 = Cl$ and $X_2, X_4 = H$

Fig. 1. Molecular Structure of *N*-(phenyl)- and *N*-(chloro substituted phenyl)-2,2-dichloroacetamides.

3. Normal co-ordinate analysis

The general molecular structure of the compounds under investigation is represented in Fig. 1.

The geometry of the all the molecules under investigation is considered by possessing C_S point group symmetry. The 51 fundamental vibrations of each compound are distributed into the irreducible representations under C_S symmetry as 36 in-plane vibrations of a' species and 15 out of plane vibrations of a'' species, i.e.,

$$\Gamma_{vib} = 36a' + 15a''$$

All vibrations are active in both IR and Raman.

Normal co-ordinate analysis provides a more quantitative description of the vibrational modes. Owing to the complexity of the molecule (51 intramolecular vibrations expected), a normal co-ordinate analysis is carried out to obtain a more complete information of the molecular motions involved in the normal modes of *N*-(phenyl)- and *N*-(chloro substituted phenyl)-2,2-dichloroacetamides, and also for a complete assignment of infrared and Raman spectra of these molecules. Wilson's FG matrix method [30–32] was used for the normal co-ordinate analysis in which the normal co-ordinates are defined with respect to a set of molecular internal co-ordinates. The normal co-ordinate calculations were performed by utilising the program of Fuhrer et al. [33] with suitable modifications for computing the G and F matrices and for adjusting a set of independent force constants. The structural parameters necessary for these compounds are taken from Sutton table [34] and structurally related similar molecules. The initial set of force constants were subsequently refined by the damped least square technique. The simple general valance force field (SGVFF) was employed for both in-plane and out of plane vibrations in order to find the potential energy distributions that are characteristics of the force field, so as to avoid any mis-assignment of frequencies, due to any possible inadequacy of force constants. The potential energy was expressed by SGVFF for the following reasons: (a) SGVFF has been shown to be very effective in normal co-ordinate analysis (NCA) of benzene and its derivatives. (b) Valence force constants can be transferred between the related molecules that are very useful in normal co-ordinate analysis [35]. All the frequencies are assigned in terms of fundamental, overtone and combination bands. To check whether the chosen set of assignments contributes maximum to the potential energy associated with the normal co-ordinates of the molecules, the potential energy distributions are calculated using the final set of force constants. The potential energy distribution corresponding to each of the observed frequencies shows the reliability and accuracy of the spectral analysis.

4. Results and discussion

The observed vibrational assignments of the compounds are discussed in four sections. The first section (Section 4.1) deals with the vibrational characteristics of *N*-(phenyl)-2,2-dichloroacetamide while the second section (Section 4.2) represents the vibrational assignments and analysis of *N*-(2-chlorophenyl)-2,2-dichloroacetamide (2CPA) and *N*-(4-chlorophenyl)-2,2-dichloroacetamide (4-CPA). The vibrational analysis of *N*-(2,3-dichlorophenyl)-2,2-dichloroacetamide (23CPA) and *N*-(2,4-dichlorophenyl)-2,2-dichloroacetamide (24CPA) are discussed in the third section (Section 4.3) and in the final section (Section 4.4), we have presented the fundamental vibrational properties of *N*-(2,3,4-trichlorophenyl)-2,2-dichloroacetamide (234CPA) and *N*-(2,4,6-trichlorophenyl)-2,2-dichloroacetamide (246-CPA).

4.1. *N-(Phenyl)-2,2-dichloroacetamide (NPA)*

The FTIR and FT-Raman spectra of *N*-(phenyl)-2,2-dichloroacetamide are shown in Figs. 2 and 3. All the observed wavenumbers are assigned in terms of fundamentals, overtones and combination bands. The observed and calculated frequencies along with their relative intensities, probable assignments and potential energy distribution of NPA are summarised in Table 2.

4.1.1. *Carbon vibrations*

The carbon–carbon stretching modes of the phenyl group are expected in the range from 1650 to 1400 cm^{-1}. Benzene has two degenerate modes at 1596 cm^{-1} (e_{2g}) and 1485 cm^{-1} (e_{1u}). Similarly the frequency of two non-degenerate modes observed at 1310 cm^{-1} (b_{2u}) and 995 cm^{-1}

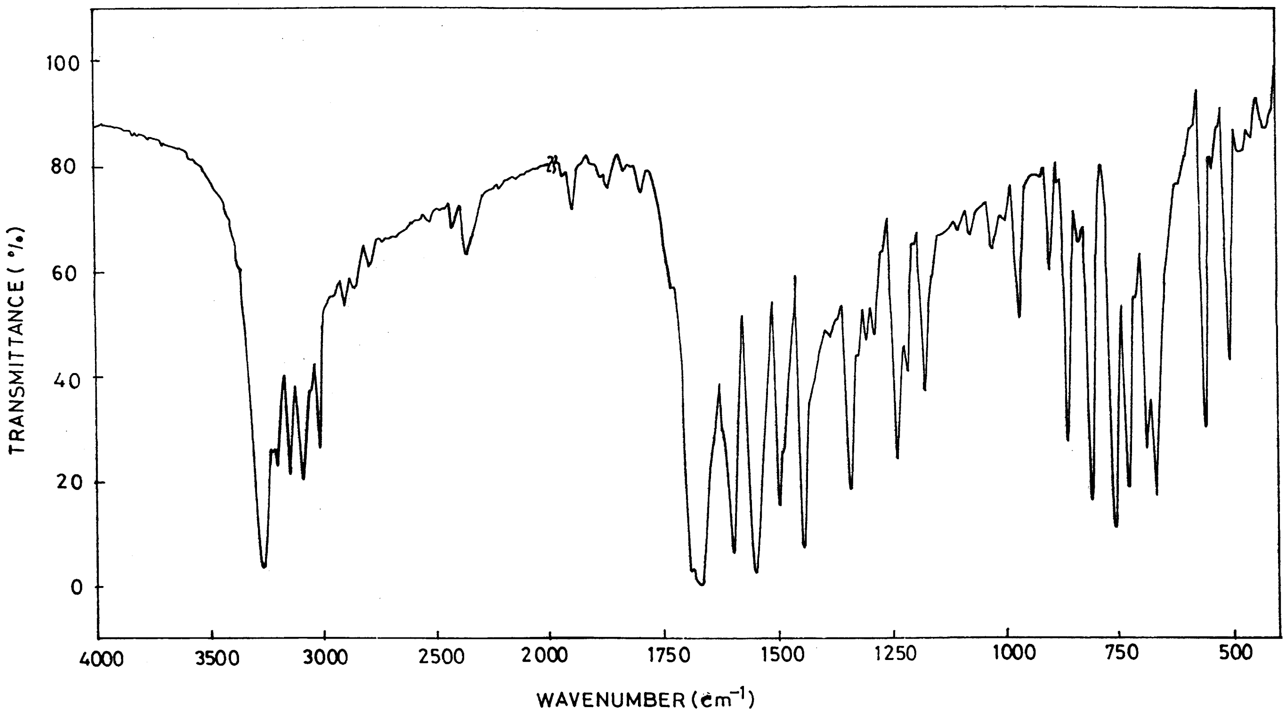

Fig. 2. FTIR spectrum of *N*-(phenyl)-2,2-dichloroacetamide.

(a_{1g}) in benzene. The actual position of these mode is determined not so much by the nature of the substituents but by the form of substitution around the ring [36]. Under C_S symmetry, in the case of NPA molecule, the C=C stretching bands appeared at 1601, 1499, 1485 cm^{-1} in the infrared and the corresponding Raman frequencies are observed at 1599, 1492, 1479 cm^{-1}. The C–C stretching modes are assigned to the bands at 1447, 1388, 1344 cm^{-1} in the IR while the respective Raman bands are observed at 1444, 1396, 1355 cm^{-1}. These frequencies appear in the respective range and the PED confirms this results and further shows that these modes are pure.

The in-plane carbon bending vibrations are obtained from the non-degenerate band at 1010 cm^{-1} (b_{1u}) and degenerate modes 606 cm^{-1} (e_{2g}) of benzene. Likewise, the CCC out of plane bending modes is defined with reference

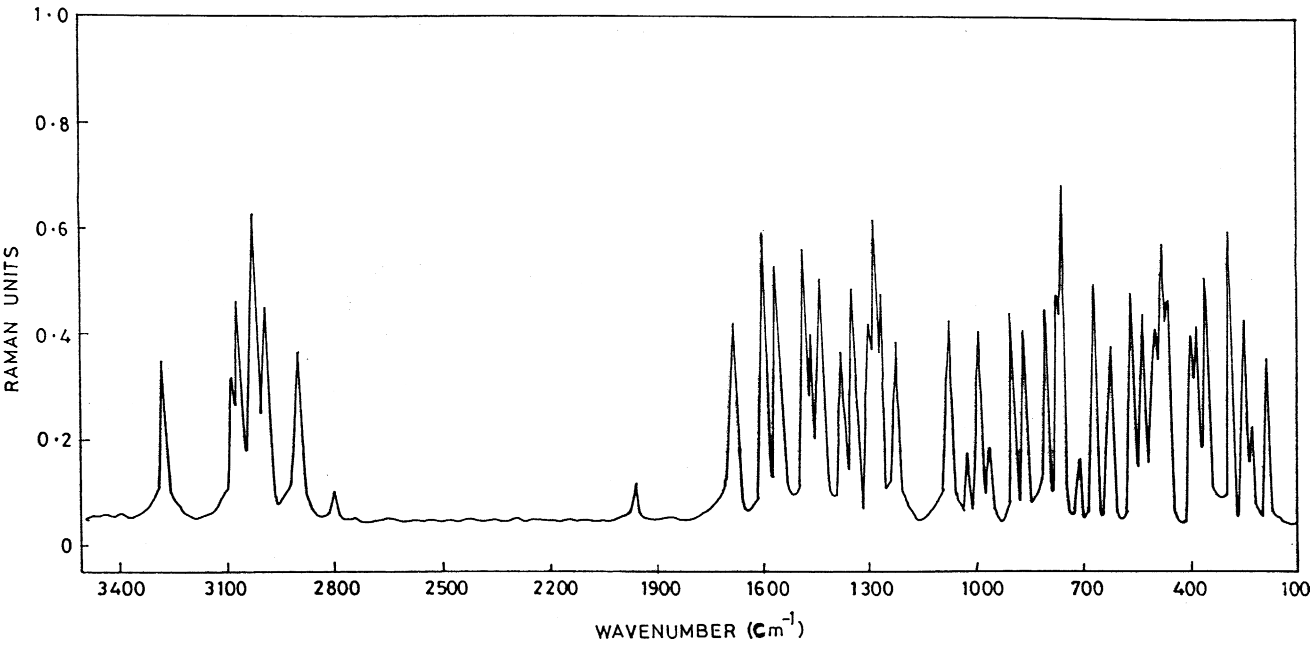

Fig. 3. FT-Raman spectrum of *N*-(phenyl)-2,2-dichloroacetamide.

Table 2
Observed and theoretical wavenumbers (cm^{-1}) and potential energy distribution (PED) for *N*-(phenyl)-2,2-dichloroacetamide[a]

Species	Observed wavenumber/int.		Calculated wavenumber	Assignment	PED (%)
	FTIR	FTR			
a'	3270 vs	3275 m	3271	N–H stretching	$97\nu_{NH}$
	3202 s	–		2 × 1601	
a'	3086 s	3087 m	3081	C–H stretching	$92\nu_{CH}$
a'	–	3063 m	3054	C–H stretching	$88\nu_{CH}$
a'	3048 w	–	3041	C–H stretching	$91\nu_{CH}$
a'	3013 s	3020 s	3017	C–H stretching	$84\nu_{CH}$
a'	2998 w	2997 m	2996	C–H stretching	$81\nu_{CH} + 11\nu_{CC}$
a'	2900 w	2900 m	2908	C–H(Cl_2) stretching	$72\nu_{CH} + 15\nu_{C–Cl}$
	2850 vw	–		2 × 1447	
	2785 vw	2795 vw		2 × 1388; 2 × 1396	
	2338 w	–		1672 + 667	
	1945 w	1952 vw		1305 + 667	
	1867 w	–		1075 + 811	
	1795 w	–		2 × 901	
a'	1672 vs	1680 m	1684	C=O stretching	$74\nu_{C=O} + 11\nu_{CN} + 10\nu_{CC}$
a'	1601 vs	1599 s	1599	C=C stretching	$84\nu_{CC}$
a'	1555 vs	1568 s	1557	N–H in-plane bending	$69\beta_{NH} + 18\beta_{CN} + 10\beta_{CCC}$
a'	1499 vs	1492 s	1494	C=C stretching	$88\nu_{CC}$
a'	1485 s	1479 m	1481	C=C stretching	$87\nu_{CC}$
a'	1447 vs	1444 s	1443	C–C stretching	$91\nu_{CC}$
a'	1388 vw	1396 m	1390	C–C stretching	$78\nu_{CC} + 14\nu_{CH}$
a'	1344 s	1355 s	1366	C–N stretching	$88\nu_{CN}$
a'			1341	C–C stretching	$74\nu_{CC} + 12\nu_{CN} + 10\nu_{CH}$
a'	1325 m	–	1311	C–C stretching	$79\nu_{CC} + 18\nu_{CH}$
a'	1305 m	1305 m	1301	C–H(Cl_2) in-plane bending	$66\beta_{CH} + 21\beta_{C–Cl}$
a'	1289 m	1292 s	1290	C–H in-plane bending	$71\beta_{CH} + 19\beta_{CCC}$
a'	1271 vw	1268 m	1274	N–C_6H_5 stretching	$59\nu_{NC} + 31\nu_{NH}$
a'	1241 s	–	1240	C–H in-plane bending	$65\beta_{CH} + 24\beta_{CCC}$
a''	1217 m	1222 m	1211	C–H(Cl_2) out of plane bending	$46\gamma_{CH} + 26\gamma_{C–Cl}$
a'	1177 m	–	1170	C–H in-plane bending	$74\beta_{CH} + 10\beta_{CCC} + 12\nu_{CC}$
a'	1075 w	1079 m	1072	C–H in-plane bending	$58\beta_{CH} + 21\beta_{CCC} + 19\nu_{CC}$
a'	1029 w	1033 w	1021	C–H in-plane bending	$62\beta_{CH} + 26\beta_{CCC}$
a'	1001 w	998 m	1000	Trigonal bending	$94\beta_{CCC}$
a''	971 m	967 w	968	C–H out of plane bending	$44\gamma_{CH} + 23\gamma_{CCC}$
a''	901 m	910 m	905	C–H out of plane bending	$51\gamma_{CH} + 22\gamma_{CCC}$
a'	861 s	870 m	860	Ring breathing	$92\beta_{CCC}$
a'	811 vs	810 m	806	C=O in-plane bending	$74\beta_{C=O} + 12\beta_{CC} + 11\beta_{CN}$
a''	–	782 m	781	C–H out of plane bending	$47\gamma_{CH} + 26\gamma_{CCC} + 14\gamma_{NH}$
a'	759 vs	760 s	764	CCl_2 asymmetric stretching	$71\nu_{C–Cl} + 18\nu_{CC} + 10\beta_{CH}$
a''	729 vs	–	719	C–H out of plane bending	$64\gamma_{CH} + 29\gamma_{CCC}$
a''	712 m	715 w	714	N–H out of plane bending	$71\gamma_{NH} + 16\gamma_{CCC}$
a''	686 s	–	687	C–H out of plane bending	$56\gamma_{CH} + 30\gamma_{CCC}$
a'	667 s	672 m	668	CCl_2 Symmetric stretching	$73\nu_{C–Cl} + 18\nu_{CH} + 10\nu_{CC}$
a'	616 vw	625 s	610	CCC in-plane bending	$66\beta_{CCC} + 18\beta_{CH}$
a''	558 s	568 m	551	C=O out of plane bending	$44\gamma_{C=O} + 28\gamma_{CC} + 10\gamma_{CN}$
a'	540 w	539 m	538	C–C in-plane bending	$54\beta_{CC} + 21\beta_{CH} + 22\beta_{CN}$
a'	505 s	511 m	507	C–N in-plane bending	$49\beta_{CN} + 29\beta_{NH}$
a'			516	CCC in-plane bending	$46\beta_{CCC} + 20\beta_{CH} + 10\nu_{CH}$
a'	479 w	483 s	468	N–C_6H_5 in-plane bending	$38\beta_{NC} + 21\beta_{NH} + 20\beta_{CN}$
a''	453 vw	457 m	450	C–N out of plane bending	$53\gamma_{CN} + 25\gamma_{C=O} + 14\gamma_{NH}$
a''	422 w	–	421	N–C_6H_5 out of plane bending	$31\gamma_{NC} + 28\gamma_{NH} + 24\gamma_{CN}$
a''	–	405 m	401	C–C out of plane bending	$58\gamma_{CC} + 31\gamma_{C–Cl} + 10\gamma_{CH}$
a''	–	384 m	371	CCC out of plane bending	$41\gamma_{CCC} + 26\gamma_{CH} + 28\gamma_{CN}$
a''	–	345 s	333	CCC out of plane bending	$38\gamma_{CCC} + 30\gamma_{CN} + 26\gamma_{CH}$
a'	–	297 s	288	CCl_2 deformation	$54\delta_{CCl_2} + 24\beta_{CH} + 11\beta_{CC}$
a''	–	253 m	256	CCl_2 twisting	$58\tau_{CCl_2} + 23\omega_{CCl_2}$
a''	–	238 w	238	CCl_2 wagging	$61\omega_{CCl_2} + 21\tau_{CCl_2}$
a'	–	195 m	191	CCl_2 rocking	$71\pi_{CCl_2} + 19\beta_{C–Cl}$

[a] vs, very strong; s, strong; m, medium; w, weak; vw, very weak, ν, stretching; δ, deformation; β, in-plane bending; γ, out of plane bending; ρ, rocking; ω, wagging; τ, twisting/torsion.

to 703 cm^{-1} (b_{2g}) and degenerate 404 cm^{-1} (e_{2u}) modes of benzene. In the present work, the bands occurring at 616, 540 and 505 cm^{-1} in the IR and 625, 539 and 511 cm^{-1} in the Raman are assigned to the CCC in-plane bending of NPA. The CCC out of plane bending modes of NPA under C_S symmetry is attributed to the Raman frequencies observed at 384 and 345 cm^{-1}. The CCC in-plane bending vibrations are described as mixed modes as there are about 20% PED contributions mainly from C–H in-plane bending and out of plane bending vibrations, respectively. The C–N in-plane and out of plane bending modes also coupled with some percentage of carbon–carbon bending vibrations.

In benzene, the ring breathing (a_{1g}) mode and the CCC trigonal bending (b_{1u}) vibrations exhibit the characteristic frequencies at 995 and 1010 cm^{-1}, respectively. In NPA, the ring breathing mode is observed at 861 cm^{-1} in the IR and 870 cm^{-1} in Raman while the CCC trigonal bending is seen at 1001 and 998 cm^{-1} in the IR and Raman, respectively. The NCA predicts that these are very pure modes since their PED contribution are almost 100%.

4.1.2. C–H vibrations

The aromatic C–H stretching vibrations are normally found between 3100 and 3000 cm^{-1}. In this region, the bands are not affected appreciably by the nature of substituents. The aromatic C–H stretching frequencies arise from the modes observed at 3062 cm^{-1} (a_{1g}), 3047 cm^{-1} (e_{2g}), 3060 cm^{-1} (b_{1u}) and 3080 cm^{-1} (e_{1u}) of benzene and its derivatives. In NPA, the phenyl C–H stretching modes are observed at 3086, 3048, 3013 and 2998 cm^{-1} in the IR and at 3087, 3063, 3020 and 2997 cm^{-1} in Raman spectra. The alkyl C–H stretching is observed in the region 3000−2850 cm^{-1}. Thus, the frequency at 2900 cm^{-1} in the IR and Raman is attributed to the C–H stretching of $-CHCl_2$ group. The PED contribution of the aromatic stretching modes indicates that these are also highly pure modes as carbon–carbon stretching, while the C–H stretching in $-CHCl_2$ group is mixed with the C–Cl stretching by 15%.

The aromatic C–H in-plane bending modes of benzene and its derivatives are observed in the region 1300−1000 cm^{-1}. Studies on the spectra of benzene shows that there are two degenerate e_{2g} (1178 cm^{-1}) and e_{1u} (1037 cm^{-1}) and two non-degenerate b_{2u} (1152 cm^{-1}) and a_{2g} (1340 cm^{-1}) vibrations involving the C–H in-plane bending. These modes are observed in NPA at 1289, 1241, 1177, 1075 and 1029 cm^{-1} in the IR and, the corresponding frequencies are obtained in the Raman at 1292, 1247, 1079 and 1033 cm^{-1}. The C–H out of plane bending mode of benzene derivatives are observed in the region 950–600 cm^{-1}. The C–H out of plane bending results from b_{2g} (985 cm^{-1}), e_{2u} (970 cm^{-1}), e_{1g} (850 cm^{-1}) and a_{2u} (671 cm^{-1}) modes of benzene. In the present case, these bands occur in the said region and are presented in Table 2. The alkyl C–H in-plane bending is assigned to the mode at 1305 cm^{-1} and the corresponding out of plane vibration is ascribed to the medium intensity band at 1217 cm^{-1} in the IR and the Raman counterpart is observed at 1222 cm^{-1}. The aromatic C–H in-plane and out of plane bending vibrations have substantial contribution from the ring CCC in-plane and out of plane bending, respectively. The alkyl C–H in-plane and out of plane bending modes are significantly overlapped with C–Cl in-plane and out of plane bending modes, respectively.

4.1.3. Amide group vibrations

A characteristic feature of the amide group in amide is the amide-I band. This mode is observed as an IR absorption peak at about 1680 cm^{-1} in *N*-phenyl acetamide. In the case of *N*-phenyl acetamide, the amide-I band is raised due to the delocalisation of the nitrogen lone pair electrons. In the *N*-phenyl acetamide structure, there is competition between the phenyl ring and the C=O for the lone pair of electrons of the nitrogen. Simple secondary amides absorbs near 1640 cm^{-1}. Amide-I band, the C=O stretching mode is the strongest band in the infrared spectrum and appears with diminished intensity in the Raman spectrum. Hence, the IR band observed at 1672 cm^{-1} is assigned to the amide-I band of NPA molecule. The Raman counterpart is obtained at 1680 cm^{-1}. The NCA shows that the amide-I band is to be pure even though it has mixed with the amide-III mode by 11% as well as 10% of C–C stretching.

The N–H in-plane bending and the C–N stretching vibrations are known as amide-II and amide-III bands, respectively. The amide-II band is often intense, almost as intense as the C=O stretch itself. The N–H in-plane bending sometimes gives rise to an overtone band at about twice the bending fundamental at around 1500 cm^{-1}. The amide-II band of NPA appeared as a very strong band at 1555 cm^{-1} in the IR and strong mode at 1568 cm^{-1} in Raman spectra. The amide-III band is strong in both IR and Raman spectra of NPA observed at 1344 cm^{-1} in the IR and 1355 cm^{-1} in Raman. Though we assigned this frequency also to C–C stretching, the NCA predicts that the potential energy contribution of C–N stretching is very high and exhibits pure in nature. The amide-II band of NPA mixes with the C–N in-plane bending to a considerable amount and the CCC in-plane bending also contributing by 10%.

The C=O in-plane bending is called the amide-IV band. In NPA molecules, it is assigned to the very strong IR band at 811 cm^{-1} and in Raman spectra at 810 cm^{-1}. The amide-V band is known as N–H out of plane bending vibration. This mode gives rise to a medium to weak band. In NPA, this mode is assigned to the wavenumber 712 and 715 cm^{-1} in the IR and Raman spectra, respectively. The C=O out of plane bending, amide-VI band of NPA which occur at 558 cm^{-1} in IR. The corresponding Raman frequency is observed at 568 cm^{-1}. The amide-IV and amide-V bands have significant contributions from C–N and C–C in-plane and out of plane bending, respectively. The N–H out of plane bending mode overlap with the ring CCC out of plane bending by 16%.

4.1.4. N–H stretching

Secondary amides are the most common and important type of amide contains only one N–H stretching band in the infrared spectrum. This band appears between 3370 and 3170 cm^{-1}. The exact location of the N–H stretching mode depends upon the other groups adjacent to the –CONH– skeleton. In more concentrated solution and in solid samples, the free N–H band is replaced by a multiple bands in the 3330−3060 cm^{-1} region. Thus, the very strong band observed at 3270 cm^{-1} in IR and in the Raman at 3275 cm^{-1} is attributed to the N–H stretching of NPA molecule. The NCA shows that this is an absolute mode.

4.1.5. C–Cl vibrations

The C–Cl absorption is observed in the broad region between 850 and 550 cm^{-1}. When several chlorine atoms are attached to one carbon atom, the band is usually more intense and at high frequency end of the assigned limits. In view of this, the very strong band in IR at 759 cm^{-1} having a strong Raman counterpart at 760 cm^{-1} is assigned to the asymmetric stretching. The symmetric CCl_2 stretching in NPA is observed at 667 cm^{-1} in IR and at 672 cm^{-1} in Raman. The in-plane CCl_2 deformation and rocking vibrations are obtained at a low frequency region of the Raman spectra corresponding to 297 and 195 cm^{-1}, respectively. The out of plane CCl_2 wagging and twisting modes are assigned to the Raman frequencies of 238 and 253 cm^{-1}, respectively. These assignments are in good agreement with the literature [37]. From the PED we observed that the asymmetric CCl_2 stretching moderately overlapped with the C–C stretch and C–H in-plane bending modes where as the symmetric CCl_2 stretching is mixed with the C–C and C–H stretching mode. CCl_2 wagging and twisting vibrations effectively mixed with each other and also the in-plane C–H and C–C bending vibrations contributed to CCl_2 deformation and rocking modes.

4.2. N-(2-Chlorophenyl)-2,2-dichloroacetamide (2CPA) and N-(4-chlorophenyl)-2,2-dichloroacetamide (4CPA)

The FTIR and FT-Raman spectra of *N*-(2-chlorophenyl)-2,2-dichloroacetamide (2CPA) and *N*-(4-chlorophenyl)-2,2-dichloroacetamide (4CPA) are presented in Figs. 4–7. The theoretical and observed wavenumbers of the fundamental vibrations of both the compounds along with their relative intensities and potential energy distribution of the individual mode is presented in Table 3. The correlation of the amide (–CONH–) group vibrational frequencies are summarised in Table 6.

4.2.1. Amide group vibrations

The N–H stretching frequency of 2CPA is found at 3255 cm^{-1} in the IR and 3253 cm^{-1} in Raman. For 4CPA, the bands at 3277 cm^{-1} in the IR and 3269 cm^{-1} in Raman are assigned to the N–H stretching vibration. By comparison, we observed that the N–H stretching of 2CPA is lowered by 20 cm^{-1} than that of NPA while there is no change in this frequency of 4CPA. In *N*-phenyl acetamide, the C=O and N–H bonds may be either *cis* or *trans* to each other. But the dipole moment measurements demonstrated

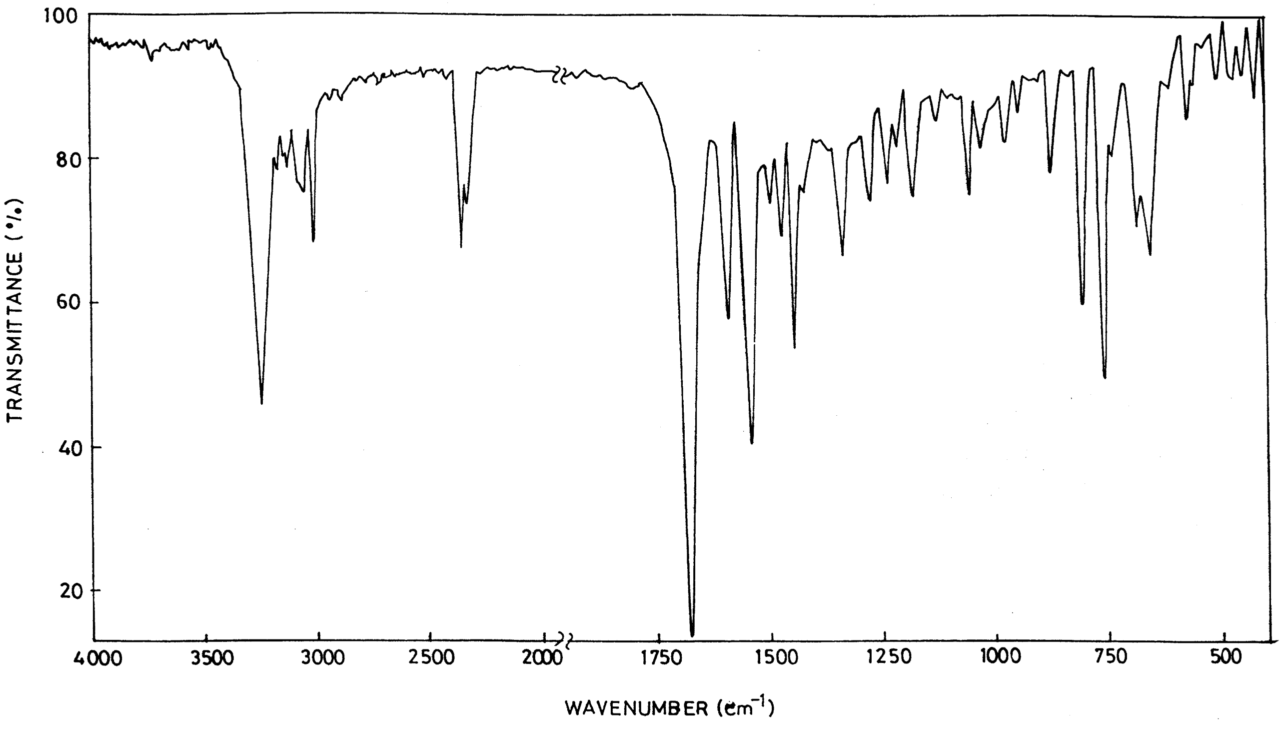

Fig. 4. FTIR spectrum of *N*-(2-chlorophenyl)-2,2-dichloroacetamide.

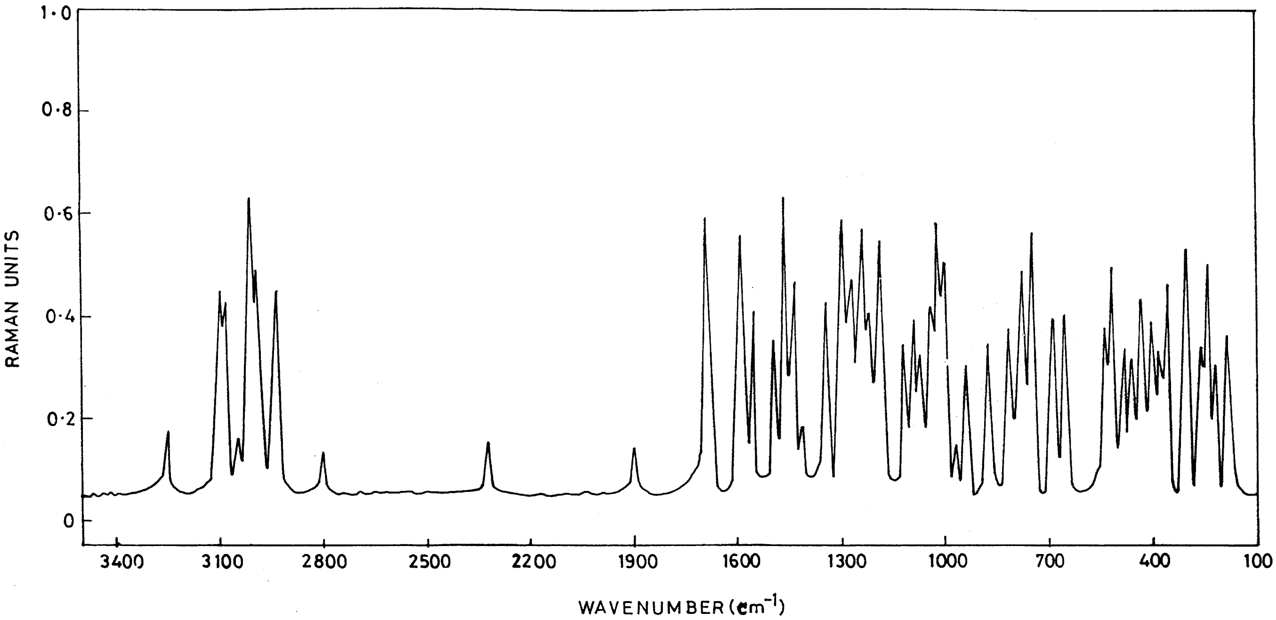

Fig. 5. FT-Raman spectrum of *N*-(2-chlorophenyl)-2,2-dichloroacetamide.

the trans conformer is the predominant and stable. Infrared spectroscopy is one of the most widely used methods to study the nature and dynamics of hydrogen bonded systems. A molecule exhibiting hydrogen bonding alters its infrared frequency in a highly dramatic fashion. Clear manifestations of hydrogen bonding are large frequency shift and band broadening of the donors hydrogen stretching vibration.

The influence of a ring substituent on N–H stretching frequency of these compounds under investigation may be the resultant of steric, direct field effect, hydrogen bonding and bond polarisation effects. In an *ortho*-chloro, bromo or nitro substituted *N*-phenyl acetamide molecules, the formation of intramolecular hydrogen bond is further favoured the trans conformation.

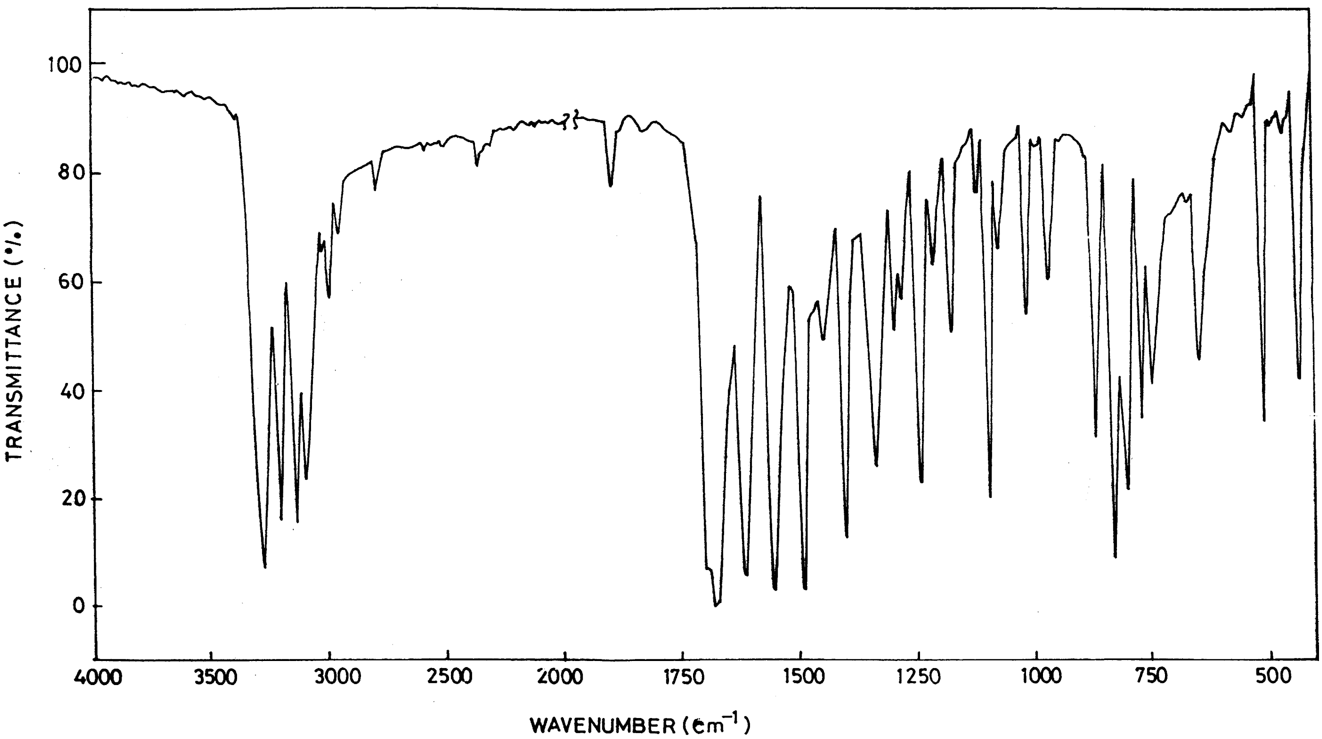

Fig. 6. FTIR spectrum of *N*-(4-chlorophenyl)-2,2-dichloroacetamide.

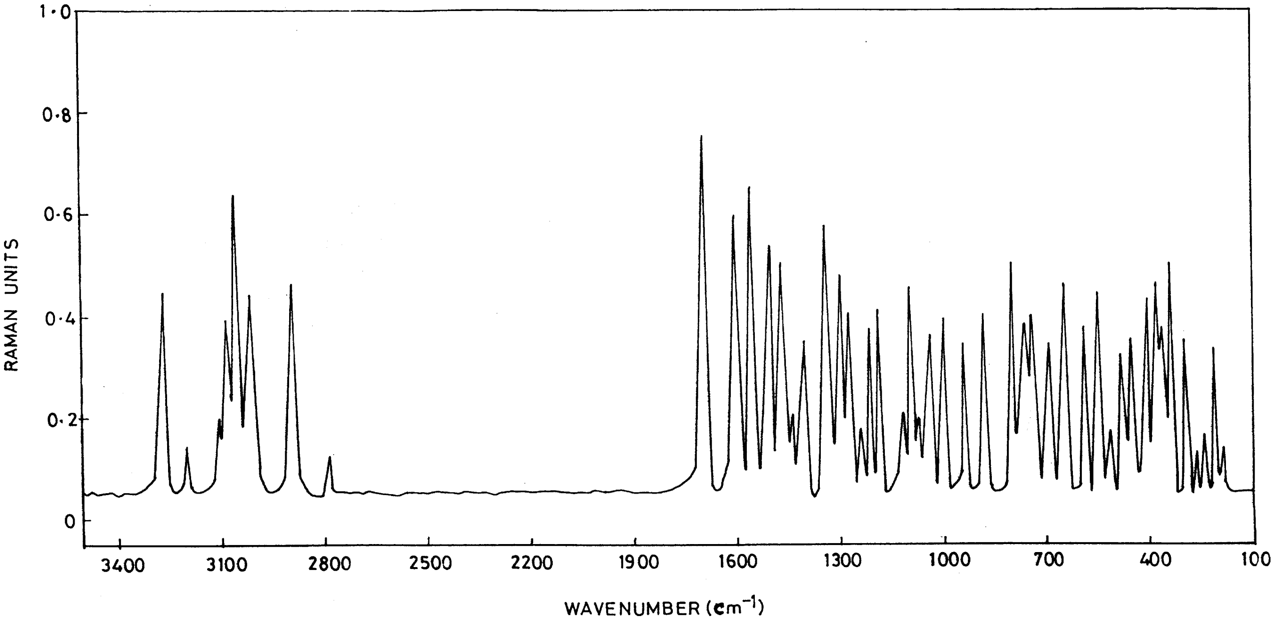

Fig. 7. FT-Raman spectrum of *N*-(4-chlorophenyl)-2,2-dichloroacetamide.

The mesomeric and inductive effects of *para* substituents have little influence on the N–H stretching vibrations of these amides and it is reasonable to assume the polarisation interactions of an *ortho* substituent, likewise, have little effect on the N–H stretching frequency [38]. The steric effect of *ortho* substituent must be considered in conjunction with the conformations. The increase in N–H stretching frequency may be expected in introduction of an *ortho* methyl or *t*-butyl group into the phenyl ring of *N*-phenyl acetamide. It is not due to the direct field effect but because of the steric interactions.

Likewise, the other *ortho* substituents chloro, bromo, nitro, methoxy groups may produce increase in N–H stretching frequency of *N*-phenyl acetamide by exerting steric compression on the N–H bond, but in addition, these substituents exerts intramolecular hydrogen bonding and also an appreciable direct field effects.

In 2CPA, the expected lowering of N–H stretching frequency is observed. This lowering of N–H frequency in 2CPA than that of NPA shows the presence of strong intramolecular hydrogen bonding between the chlorine atom connected at the *ortho* position and the hydrogen of the amide group. The intramolecular hydrogen bonding is considered to be the predominant effect than the steric factor. Steric compressions and the direct field effects exerted by *ortho* substituents may offset the depression.

The amide-I band of 2CPA is found at 1678 cm^{-1} in IR and 1685 cm^{-1} in Raman while in 4CPA the corresponding frequencies are observed at 1676 and 1682 cm^{-1}. The increase in wavenumber of C=O stretching in 2CPA and 4CPA than that of NPA molecule reveals that the substitution of chlorine in the phenyl ring makes the molecule effectively compete with the carbonyl oxygen for the electrons of the nitrogen, thus increasing the force constants of the C=O bond.

The frequencies observed at 1545 and 1555 cm^{-1} in IR are ascribed to the amide-II band of 2CPA and 4CPA, respectively. The corresponding Raman counterpart obtained at 1551 and 1558 cm^{-1}. The C–N stretching modes of 2CPA is assigned at 1340 and 1346 cm^{-1} in IR and Raman spectra. The strong fundamental modes observed at 1338 and 1350 cm^{-1} in IR and Raman is attributed to C–N stretching of 4CPA. The amide-IV, C=O in-plane bending of 2CPA is found at 807 cm^{-1} in IR and 804 cm^{-1} in Raman. The fundamental modes 801 and 800 cm^{-1} are attributed to the C=O in-plane bending of 4CPA molecule. The amide-V, the N–H out of plane bending is observed at 739, 742 cm^{-1} in 2CPA and at 745, 749 cm^{-1} in 4CPA. The C=O out of plane bending of 2CPA is seen at 574 cm^{-1} in IR, the corresponding frequency of 4CPA is observed at 574 and 584 cm^{-1} in IR and Raman spectra.

The other amide group vibrations of 2CPA and 4CPA molecules exhibit their characteristics in a similar fashion. When compared these modes of 2CPA and 4CPA with that of the amide group frequencies of NPA molecule, no appreciable changes in the magnitude of these modes are observed except the N–H out of plane bending mode. The amide-V, mode of 2CPA and 4CPA is shifted to higher frequency by 30 cm^{-1} than in NPA. The PED calculations determine that the amide-I, amide-II, amide-IV and amide-VI bands possessing the character of C–N and C–C vibrations. The amide-III and amide-V bands are significantly overlapped with the N–H stretching and CCC out of plane bending vibrations.

4.2.2. Carbon vibrations

The frequency of e_{2g} degenerate pair in benzene is fairly insensitive to substitution. Similarly, the frequency of e_{1u} vibrations pair is also not very sensitive to substitution,

Table 3
Observed and theoretical wavenumbers (cm^{-1}) and potential energy distribution (PED) for *N*-(2-chlorophenyl)- and *N*-(4-chlorophenyl)-2,2-dichloroacetamides[a]

Species	Observed wavenumber/int.				Calculated wavenumber	Assignment	PED (%)
	N-(2-Chlorophenyl)-2, 2-dichloroacetamide		*N*-(4-Chlorophenyl)-2, 2-dichloroacetamide				
	FTIR	FTR	FTIR	FTR			
a′	3255 s	3253 w	3277 vs	3269 m	3258	N–H stretching	$95\nu_{NH}$
	–	–	3207 s	3201 w		2 × 1617; 2 × 1600	
	3176 w	–	–	–		2 × 1588	
a′	3104 w	3100 m	3106 s	3104 w	3101	C–H stretching	$91\nu_{CH}$
a′	–	3086 m	3094 s	3091 m	3085	C–H stretching	$88\nu_{CH}$
a′	3052 m	3045 w	–	3057 s	3044	C–H stretching	$94\nu_{CH}$
a′	3011 m	3009 s	–	3000 m	3002	C–H stretching	$84\nu_{CH} + 11\nu_{CC}$
	–	2992 m	2986 m	–		2 × 1499; 2 × 1492	
a′	2889 w	2892 m	2891 w	2886 m	2881	C–H(Cl$_2$) stretching	$84\nu_{CH} + 10\nu_{C–Cl}$
	–	–	2853 vw	–		1555 + 1419	
	–	2796 vw	2793 w	2789 vw	–	1676 + 1098; 1682 + 1100	
	2360 m	–	2360 w	–		1678 + 684; 1676 + 687	
	2337 m	2346 w	–	–		1551 + 804; 1545 + 807	
	–	1905 w	1892	–		1095 + 804; 1098 + 801	
a′	1678 vs	1685 s	1676 vs	1682 vs	1681	C=O stretching	$71\nu_{C=O} + 14\nu_{CN} + 10\nu_{CC}$
a′	1593 m	1591 s	1617 vs	1600 s	1599	C=C stretching	$90\nu_{CC}$
a′	1545 vs	1551 m	1555 vs	1558 vs	1542	N–H in-plane bending	$61\beta_{NH} + 16\beta_{CN} + 10\beta_{CC}$
a′	1500 w	1499 m	1492 vs	1501 s	1500	C=C stretching	$80\nu_{CC}$
a′	1475 m	1471 s	–	1472 s	1467	C=C stretching	$74\nu_{CC}$
a′	1446 s	1449 m	1447 m	1441 w	1442	C–C stretching	$91\nu_{CC}$
a′	1425 vw	1422 w	1419 s	1415 m	1421	C–C stretching	$68\nu_{CC} + 24\nu_{C–Cl}$
a′	1340 m	1346 m	1338 s	1350 s	1338	C–N stretching	$61\nu_{CN} + 21\nu_{NH}$
a′						C–C stretching	$64\nu_{CC} + 28\nu_{CN}$
a′	–	1299 s	1296 m	1294 s	1292	C–C stretching	$61\nu_{CC} + 24\nu_{CH}$
a′	1280 m	1271 m	1281 m	1273 m	1271	N–C$_6$H$_5$ stretching	$54\nu_{NC} + 24\nu_{CH}$
a′	1238 m	1241 s	1241 s	1242 w	1233	C–H(Cl$_2$) in-plane bending	$68\beta_{CH} + 26\beta_{CC}$
a″	1217 w	1225 m	1213 m	1219 m	1220	C–H(Cl$_2$) out of plane bending	$38\gamma_{CH} + 30\gamma_{C–Cl}$
a′	1181 m	1189 s	1177 s	1187 m	1174	C–H in-plane bending	$72\beta_{CH} + 14\beta_{CCC}$
a′	1128 w	1130 m	1119 w	1121 w	1118	C–H in-plane bending	$56\beta_{CH} + 30\beta_{CCC}$
a′	–	1095 m	1098 vs	1100 s	1094	C–H in-plane bending	$61\beta_{CH} + 26\beta_{CCC}$
a′	–	1070 m	1075 m	1073 w	1072	C–H in-plane bending	$70\beta_{CH} + 24\beta_{CCC}$
a″	1059 m	1052 m	–	1050 m	1051	C–H out of plane bending	$41\gamma_{CH} + 26\gamma_{CCC}$
a″	1034 w	1037 s	1034 vw	–	1032	C–H out of plane bending	$54\gamma_{CH} + 20\gamma_{CCC}$
a′	–	1007 s	1015 m	1009 m	1009	Trigonal bending	$96\beta_{CCC}$
a″	975 m	971 vw	967 m	–	970	C–H out of plane bending	$47\gamma_{CH} + 26\gamma_{CCC} + 20\gamma_{NH}$
a″	944 w	939 m	–	935 m	941	C–H out of plane bending	$62\gamma_{CH} + 23\gamma_{CCC}$
a′	873 m	879 m	866 s	880 m	870	Ring breathing	$94\beta_{CCC}$
a′	807 s	804 m	801 vs	800 s	806	C=O in-plane bending	$61\beta_{C=O} + 11\beta_{CC} + 14\beta_{CN}$
a′	760 vs	779 m	767 s	770 m	766	CCl$_2$ asymmetric stretching	$76\nu_{C–Cl} + 22\nu_{CC}$
a″	739 m	742 s	745 s	749m	743	N–H out of plane bending	$74\gamma_{NH} + 12\gamma_{CCC}$
a′	684 m	687 m	–	690 m	681	C–Cl stretching	$69\nu_{C–Cl} + 16\nu_{CC}$
a′	655 s	657 m	640 s	648 s	652	CCl$_2$ Symmetric stretching	$69\nu_{C–Cl} + 20\nu_{CC} + 10\nu_{CH}$
a″	574 m	–	574 vw	584 m	585	C=O out of plane bending	$40\gamma_{C=O} + 21\gamma_{CC} + 18\gamma_{CN}$
a′					580	CCC in-plane bending	$45\beta_{CCC} + 20\beta_{CH} + 26\beta_{NC}$
a′	–	545 m	552 vw	556 s	551	C–C in-plane bending	$48\beta_{CC} + 24\beta_{CH} + 26\beta_{CN}$
a′	–	515 s	509 s	518 w	510	C–N in-plane bending	$51\beta_{CN} + 32\beta_{NH}$
a′	–	483 m	490 vw	487 m	485	CCC in-plane bending	$49\beta_{CCC} + 25\beta_{CH} + 24\beta_{CN}$
a″	–	459 m	467 w	462 m	461	C–N out of plane bending	$51\gamma_{CN} + 30\gamma_{C=O} + 10\gamma_{NH}$
a′	422 w	430 s	433 s	–	430	N–C$_6$H$_5$ in-plane bending	$38\beta_{NC} + 21\beta_{NH} + 21\beta_{CN}$
a″	–	402 m	–	407 s	401	C–C out of plane bending	$31\gamma_{CC} + 20\gamma_{C=O} + 16\gamma_{C–Cl}$
a″	–	381 m	–	385 s	378	N–C$_6$H$_5$ out of plane bending	$28\gamma_{NC} + 21\gamma_{NH} + 21\gamma_{NC}$
a″					367	CCC out of plane bending	$38\gamma_{CCC} + 24\gamma_{CH} + 16\gamma_{CN}$
a″	–	364 s	–	360 m	361	CCC out of plane bending	$40\gamma_{CCC} + 28\gamma_{CH} + 18\gamma_{CN}$
a′	–	341 s	–	339 s	344	C–Cl in-plane bending	$49\beta_{C–Cl} + 29\beta_{CH} + 24\beta_{CC}$
a′	–	301 m	–	305 m	306	CCl$_2$ deformation	$51\delta_{CCl_2} + 20\beta_{CH} + 11\beta_{CC}$
a″	–	260 m	–	263 w	261	CCl$_2$ twisting	$51\tau_{CCl_2} + 29\omega_{CCl_2}$
a″	–	245 s	–	242 w	244	CCl$_2$ wagging	$48\omega_{CCl_2} + 31\tau_{CCl_2}$
a″	–	222 m	–	219 m	220	C–Cl out of plane bending	$39\gamma_{C–Cl} + 24\gamma_{C=O} + 22\gamma_{CH}$
a′	–	185 m	–	180 w	181	CCl$_2$ rocking	$65\pi_{CCl_2} + 29\delta_{CCl_2}$

[a] vs, very strong; s, strong; m, medium; w, weak; vw, very weak, ν, stretching; δ, deformation; β, in-plane bending; γ, out of plane bending; ρ, rocking; ω, wagging; τ, twisting/torsion.

although heavy halogens cause undoubtedly diminish the frequency [39]. The C=C stretching of 2CPA is found in the IR spectrum at 1593, 1500, 1475 cm^{-1} and at 1591, 1499, 1471 cm^{-1} in Raman. Similarly, the very strong lines observed in the infrared spectrum of 4CPA at 1617, 1492 cm^{-1} and in the Raman at 1600, 1501, 1472 cm^{-1} are ascribed to the C=C stretching modes. The C–C modes of 2CPA and 4CPA are given Table 3. These are all considered to be absolute modes according to the normal co-ordinate analysis.

4.2.3. C–H vibrations

The C–H present in the phenyl ring of 2CPA gives bands at 3104, 3052, 3011 cm^{-1} in IR and at 3100, 3086, 3045, 3009 cm^{-1} in Raman. In 4CPA, these modes are obtained as strong bands in IR at 3106 and 3094 cm^{-1} while in Raman these are observed at 3104, 3091, 3057 and 3000 cm^{-1}. The alkyl C–H stretching frequency of 2CPA and 4CPA is observed at 2889, 2891 cm^{-1} in IR and 2892, 2886 cm^{-1} in Raman, respectively. All other in-plane and out of plane bending vibrations of C–H mode is presented in Table 3.

4.2.4. C–Cl vibrations

Three frequencies are expected in the region 800–550 cm^{-1}, whose origin can be attributed to the stretching vibrations of CCl_2 group and the phenyl C–Cl bond. The asymmetric stretching mode of CCl_2 in 2CPA is observed at 760 cm^{-1} in IR and 779 cm^{-1} in Raman. Strong infrared band at 655 cm^{-1} and medium Raman band at 657 cm^{-1} are ascribed to the symmetric CCl_2 stretching mode of 2CPA. In 4CPA, the bands at 767, 770 cm^{-1} and 640, 648 cm^{-1} are attributed to the asymmetric and symmetric CCl_2 stretching vibrations, respectively. The phenyl C–Cl stretching mode of 2CPA is observed as a medium band at 684 cm^{-1} in IR and 687 cm^{-1} in Raman, whereas in 4CPA it is found only in Raman at 690 cm^{-1}. The strong Raman bands at 341 and 339 cm^{-1} are assigned to the C–Cl in-plane bending whereas the out of plane bending is assigned to the medium bands observed at 222 and 219 cm^{-1} in Raman for 2CPA and 4CPA, respectively. The other vibrations of CCl_2 like deformation, rocking, wagging and twisting modes of 2CPA and 4CPA are observed in the similar region as in the case of NPA molecule and are presented in Table 3. The contribution of the corresponding C–Cl vibrations observed about 70% and hence these modes are also pure modes. In the low frequency region of the infrared and Raman spectra of 2CPA and 4CPA, mainly the C–Cl in-plane and out of plane bending modes are extensively mixed with other modes.

4.3. *N*-(2,3-Dichlorophenyl)-2,2-dichloroacetamide (23CPA) and *N*-(2,4-dichlorophenyl)-2,2-dichloroacetamide (24CPA)

The FTIR and FT-Raman spectra of *N*-(2,3-dichlorophenyl)-2,2-dichloroacetamide and *N*-(2,4-dichlorophenyl)-2,2-dichloroacetamide are shown in Figs. 8–11. The vibrational assignments of these compounds are made on the basis of observed frequencies and their relative intensities in FTIR and FT-Raman spectra together and potential energy distribution of the fundamental frequencies calculated from the normal co-ordinate analysis are presented in Table 4.

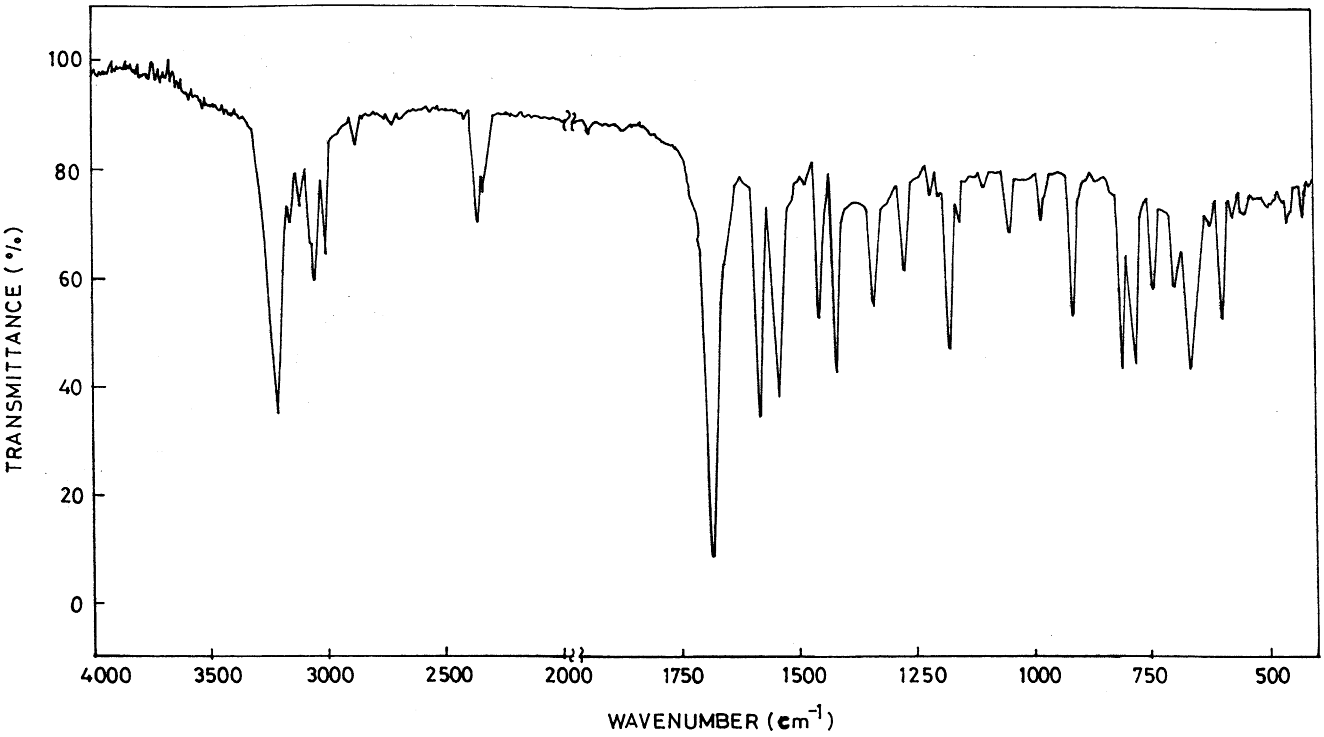

Fig. 8. FTIR spectrum of *N*-(2,3-dichlorophenyl)-2,2-dichloroacetamide.

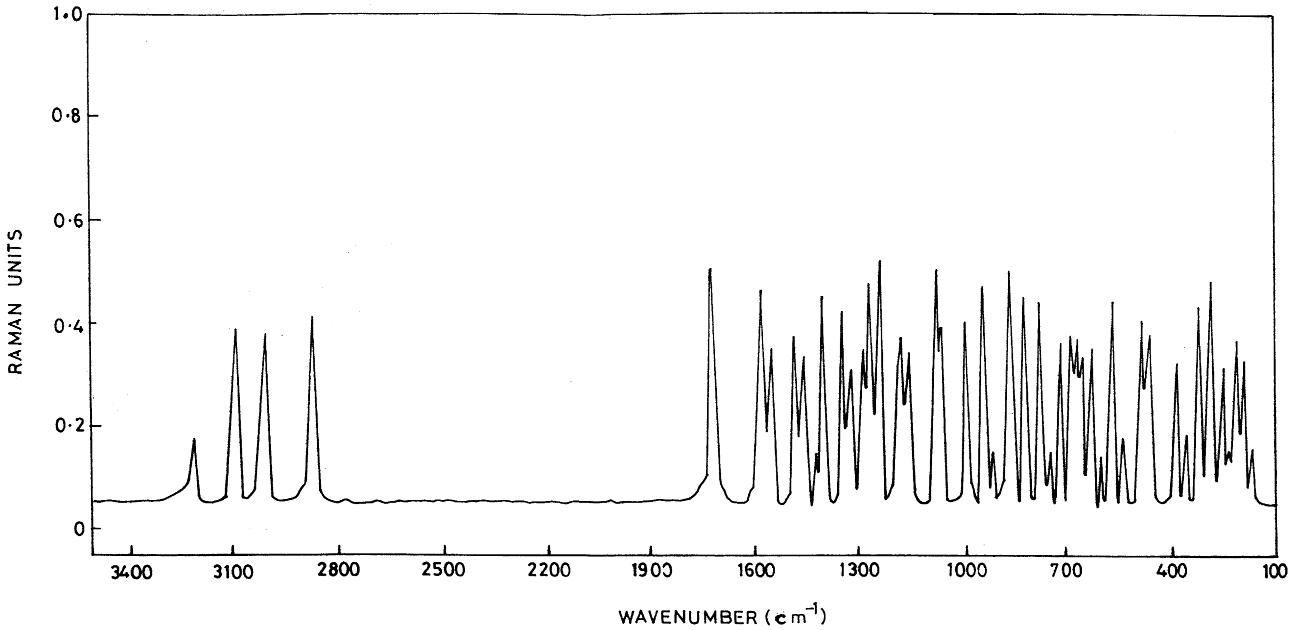

Fig. 9. FT-Raman spectrum of *N*-(2,3-dichlorophenyl)-2,2-dichloroacetamide.

4.3.1. *N–H stretching*

The strong IR band observed at 3218 cm^{-1} and a weak Raman band at 3215 cm^{-1} is assigned to the N–H stretching mode of 23CPA. In 24CPA, the N–H stretching mode is attributed to the medium band at 3199 cm^{-1} in infrared and 3210 cm^{-1} in Raman. The N–H stretching of 24CPA is shifted to lower frequency by 15 cm^{-1} when compared to 23CPA. The N–H stretching frequency of 23CPA and 24CPA molecules are significantly lowered than the monochloro substituted compounds and NPA by around 50 cm^{-1} confirm the presence of intramolecular hydrogen bonding.

4.3.2. *Amide group vibrations*

The C=O stretching of 23CPA and 24CPA are observed at 1684, 1682 cm^{-1} in infrared and 1680, 1685 cm^{-1} in Raman spectra, respectively. The amide-II, amide-III, amide-IV and amide-VI vibrations of 23CPA and 24CPA are observed as almost equal in magnitudes and also not deviated much from

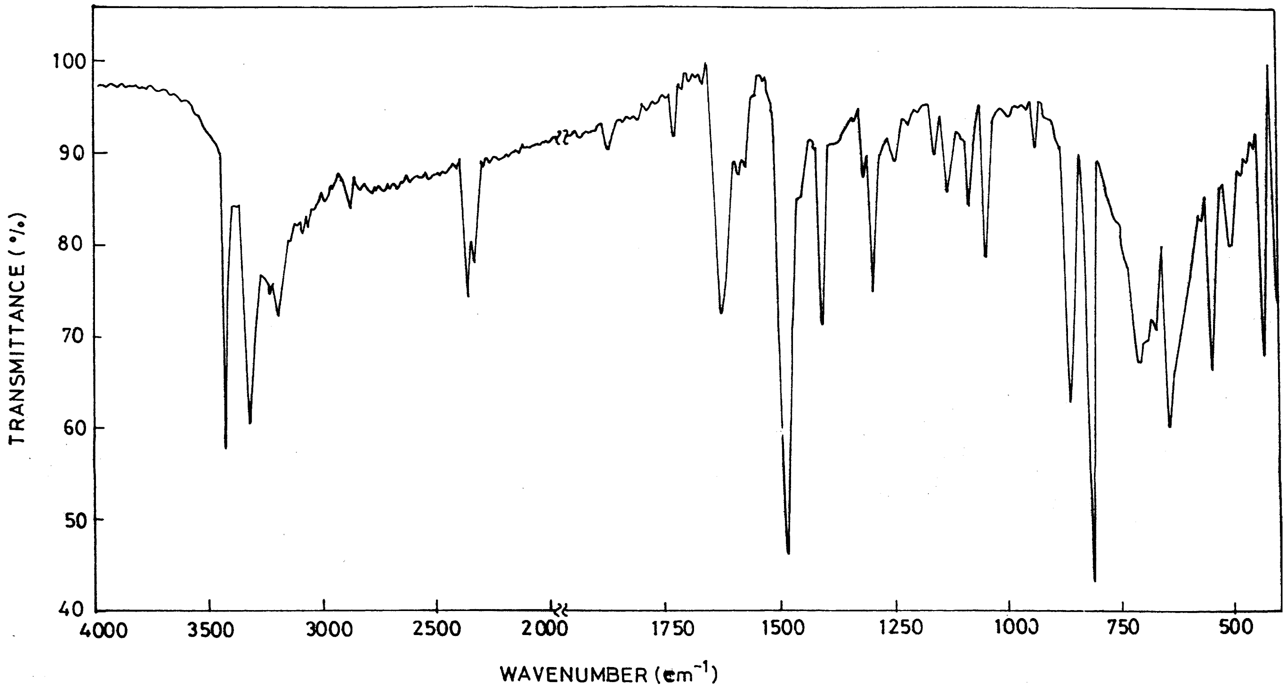

Fig. 10. FTIR spectrum of *N*-(2,4-dichlorophenyl)-2,2-dichloroacetamide.

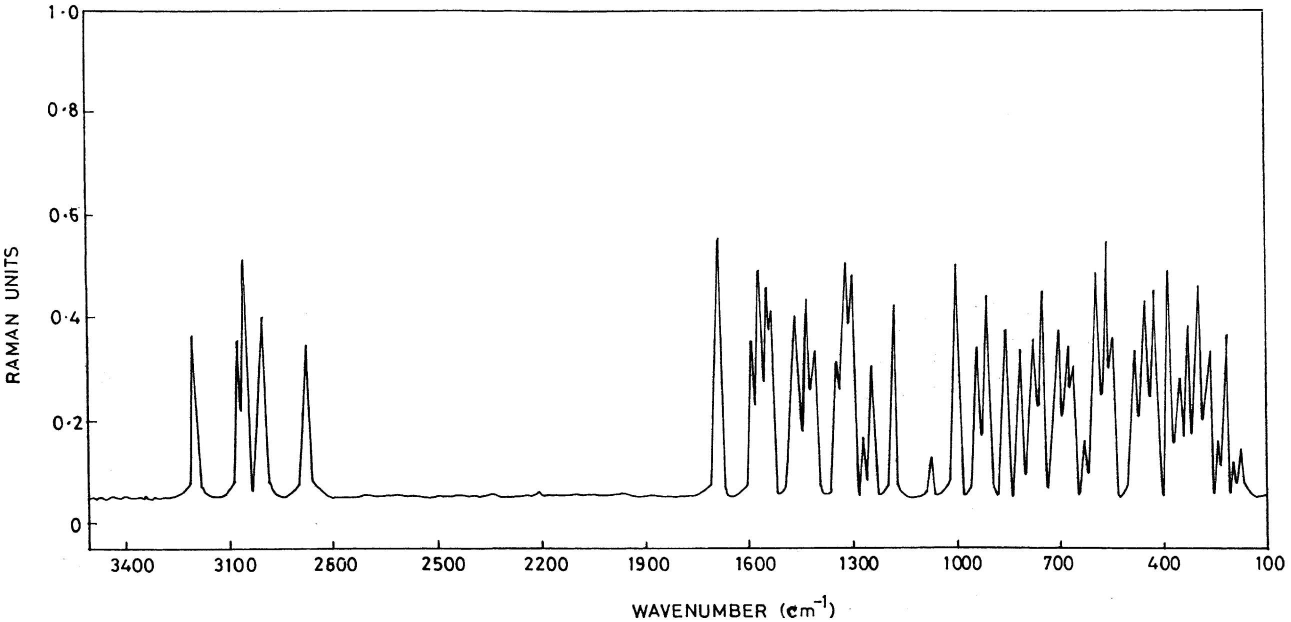

Fig. 11. FT-Raman spectrum of *N*-(2,4-dichlorophenyl)-2,2-dichloroacetamide.

the corresponding frequencies of NPA. The N–H out of plane bending of 23CPA and 24CPA produce significant frequency shift from that of NPA. It has 14% contribution from CCC out of plane bending vibrations.

4.3.3. C–Cl vibrations

The C–Cl stretching of 23CPA and 24CPA are found in the expected range. The frequencies seen at 694 cm^{-1} in infrared and 715, 689 cm^{-1} in Raman are ascribed to the C–Cl stretching in 23CPA while in 24CPA it is observed at 707, 692 cm^{-1} in IR and 704, 687 cm^{-1} in Raman, respectively. The CCl_2 asymmetric and symmetric stretching frequencies of 23CPA and 24CPA does not show any variation from that of the corresponding frequencies in NPA. The CCl_2 wagging mode significantly overlap with CCl_2 twisting mode and vice versa. Similarly the aromatic C–Cl out of plane bending modes also have more than 20% CCC out of plane bending contribution. The NCA shows that C–N, N–C and CCC out of plane bending vibrations strongly coupled with other modes and the original character of the respective mode is only about 50%.

4.4. N-(2,3,4-Trichlorophenyl)-2,2-dichloroacetamide (234CPA) and N-(2,4,6-trichlorophenyl)-2,2-dichloroacetamide (246CPA)

The Figs. 12–15 represent the FTIR and FT-Raman spectra of 234CPA and 246CPA. The observed and calculated vibrational frequencies, the assignments of different vibrational fundamental modes and the potential energy contribution of the individual modes are given in Table 5. The results presented in Table 5 are self explanatory. Hence the discussion is confined mainly to the vibrations having their origin in –CONH– moiety and carbon vibrations. The C=C stretching modes of 234CPA are observed in IR at 1531 and 1445 cm^{-1} while in Raman these are ascribed to the frequencies 1535, 1449 and 1429 cm^{-1}. In 246CPA, the C=C fundamental modes are assigned to the frequencies of 1532, 1453, 1432 cm^{-1} in IR and the Raman counterpart at 1535, 1447 and 1430 cm^{-1}. Similarly, the C–C stretching modes of 234CPA are obtained at 1393, 1371, 1330 cm^{-1} in the infrared, the corresponding Raman frequencies are assigned at 1389, 1368, 1328 cm^{-1}. In 246CPA, these modes are observed at 1392, 1374, 1332 and 1398, 1368, 1331 cm^{-1} in the infrared and Raman spectra, respectively. Although the carbon–carbon vibrations are considered to be fairly insensitive to the substitutions in the phenyl ring these cause decrease in frequency by heavy halogen substitution. In the cases of 234CPA and 246CPA, the frequency of carbon–carbon stretching shifted to lower frequency side when compared to other compounds studied in the present work. That is, the carbon–carbon stretching modes vary from 1601 to 1325 cm^{-1} in the infrared of NPA while in Raman from 1599 to 1355 cm^{-1}. But in the case of 234CPA and 246CPA the range of these modes are obtained between 1531 and 1272 and, 1532−1254 cm^{-1} in the infrared, respectively. Similar trends are also noticed in the Raman spectra of 234CPA and 246CPA. Thus, the vibrational bands corresponding to the e_{2g} mode of benzene and its derivatives, which appears at 1596 cm^{-1}, and the e_{1u} mode at 1485 cm^{-1} are lowered in these chloro substituted *N*-phenyl acetamide and is very significantly pronounced in 234CPA and 246CPA.

The aromatic C–H stretching modes of 234CPA are obtained at 3069 and 3017 cm^{-1} in IR and, 3075 and 3025 cm^{-1} in Raman. Likewise, the strong modes present at 3077, 3030

Table 4
Observed and theoretical wavenumbers (cm^{-1}) and potential energy distribution (PED) for *N*-(2,3-dichlorophenyl)- and *N*-(2,4-dichlorophenyl)-2,2-dichloroacetamides[a]

Species	Observed wavenumber/int.				Calculated wavenumber	Assignment	PED (%)
	N-(2,3-Dichlorophenyl))-2, 2-dichloroacetamide		*N*-(2,4-Dichlorophenyl)-2, 2-dichloroacetamide				
	FTIR	FTR	FTIR	FTR			
	–	–	3418 s	–		2870 + 548	
	–	–	3317 s	–		2 × 1682	
a′	3218 s	3215 w	3199 m	3210 m	3211	N–H stretching	$96\nu_{NH}$
	3157 w	–	–	–		2 × 1583	
	3114 w	–	–	–		1684 + 1420	
a′	–	3084 m	3075 s	3078 m	3074	C–H stretching	$90\nu_{CH}$
a′	3054 m	–	3060 w	3055 s	3055	C–H stretching	$88\nu_{CH}$
a′	3009 m	3007 m	–	3005 m	3007	C–H stretching	$94\nu_{CH}$
a′	2887 vw	2871 m	2870 vw	2877 m	2885	C–H(Cl_2) stretching	$81\nu_{CH} + 10\nu_{CC} + 11\nu_{CN}$
	2360 m	–	2361 m	–		2 × 1179; 1569 + 812	
	2338 w	–	2336 m	–		1684 + 662; 1682 + 670	
	–	–	1805 w	–		1291 + 548	
	–	–	1720 w	–		1000 + 707	
a′	1684 vs	1680 s	1682 m	1685 s	1681	C=O stretching	$75\nu_{C=O} + 16\nu_{CN}$
a′	1583 s	1582 s	1592 m	1589 m	1584	C=C stretching	$91\nu_{CC}$
a′	1562 s	–	1569 m	1567 s	1569	N–H in-plane bending	$72\beta_{NH} + 16\beta_{CN} + 12\beta_{CC}$
a′	1542 s	1548 m	–	1545 s	1541	C=C stretching	$88\nu_{CC}$
a′	1483 vw	1485 m	1481 vs	–	1480	C=C stretching	$79\nu_{CC}$
a′	1454 m	1454 m	–	1462 s	1458	C–C stretching	$84\nu_{CC}$
a′	1420 s	1427 w	–	1430 s	1428	C–C stretching	$92\nu_{CC}$
a′	–	1409 s	1400 s	1405 m	1410	C–C stretching	$81\nu_{CC} + 12\nu_{CH}$
a′	1340 m	1345 s	–	1342 m	1342	C–N stretching	$88\nu_{CN}$
a′	–	1322 m	1315 w	1320 s	1314	C–C stretching	$69\nu_{CC} + 18\nu_{CH}$
a′	–	1298 m	1291 s	1293 s	1287	C–H(Cl_2) in-plane bending	$61\beta_{CH} + 23\beta_{C-Cl}$
a′	1273 m	1267 s	–	1273 w	1261	N–C_6H_5 stretching	$54\nu_{NC} + 28\nu_{NH}$
a″	–	1237 s	1244 w	1242 m	1240	C–H(Cl_2) out of plane bending	$42\gamma_{CH} + 28\gamma_{C-Cl}$
a′	1179 s	1178 m	–	1184 s	1180	C–H in-plane bending	$81\beta_{CH} + 10\beta_{CCC}$
a′	1158 w	1152 m	1153 m	–	1151	C–H in-plane bending	$74\beta_{CH} + 11\nu_{CC} + 10\beta_{CCC}$
a′	–	1074 s	1081 m	1079 vw	1072	C–H in-plane bending	$65\beta_{CH} + 29\beta_{CCC}$
a″	1051 m	1060 m	1044 m	–	1041	C–H out of plane bending	$41\gamma_{CH} + 28\gamma_{CCC}$
a′	983 w	992 m	1000 w	998 s	994	Trigonal bending	$96\beta_{CCC}$
a″	–	937 s	931 vs	940 m	940	C–H out of plane bending	$61\gamma_{CH} + 31\gamma_{CCC}$
a″	913 m	909 w	–	917 s	910	C–H out of plane bending	$55\gamma_{CH} + 28\gamma_{NH}$
a′	–	865 s	861 s	855 m	858	Ring breathing	$94\beta_{CCC}$
a′	809 s	816 s	812 vs	815 m	814	C=O in-plane bending	$69\beta_{C=O} + 14\beta_{CC} + 12\beta_{CH}$
a′	781 s	779 s	775 vs	774 m	780	CCl_2 asymmetric stretching	$72\nu_{C-Cl} + 17\nu_{CC}$
a″	740 m	749 w	–	752 s	751	N–H out of plane bending	$74\gamma_{NH} + 14\gamma_{CCC}$
a′	–	715 m	707 s	704 m	710	C–Cl stretching	$69\nu_{C-Cl} + 20\beta_{CCC}$
a′	694 m	689 m	692 m	–	689	C–Cl stretching	$71\nu_{C-Cl} + 10\beta_{CCC}$
a′	662 s	667 m	670 m	672 m	671	CCl_2 Symmetric stretching	$68\nu_{C-Cl} + 11\beta_{CH} + 15\beta_{CC}$
a′	–	651 m	643 s	659 m	648	CCC in-plane bending	$64\beta_{CCC} + 15\beta_{CH}$
a′	621 vw	627 m	–	625 w	626	CCC in-plane bending	$69\beta_{CCC} + 21\beta_{CH}$
a′	595 m	593 w	–	597 s	594	CCC in-plane bending	$58\beta_{CC} + 18\beta_{CH} + 11\beta_{CN}$
a″	573 vw	571 s	570 vw	567 s	563	C=O out of plane bending	$41\gamma_{C=O} + 21\gamma_{CC} + 11\gamma_{CN}$
a′	551 vw	545 w	548 s	549 m	543	CN in-plane bending	$53\beta_{CN} + 30\beta_{NH}$
a′	–	481 s	470 vw	480 m	474	N–C_6H_5 in-plane bending	$41\beta_{NC} + 18\beta_{NH} + 21\beta_{CN}$
a″	455 vw	459 s	–	450 s	451	C–N out of plane bending	$51\gamma_{CN} + 20\gamma_{C=O} + 18\gamma_{NH}$
a″						CC out of plane bending	$38\gamma_{CC} + 26\gamma_{C-Cl} + 21\gamma_{CH}$
a″	425 vw	–	434 s	427 s	428	CCC out of plane bending	$44\gamma_{CCC} + 21\gamma_{CH} + 20\gamma_{CN}$
a″	–	385 m	–	389 s	381	N–C_6H_5 out of plane bending	$30\gamma_{NC} + 24\gamma_{NH} + 21\gamma_{NC}$
a″						CCC out of plane bending	$38\gamma_{CCC} + 22\gamma_{CN} + 21\gamma_{CH}$
a′	–	355 w	–	352 m	350	C–Cl in-plane bending	$64\beta_{C-Cl} + 21\beta_{CCC}$
a′	–	322 s	–	327 m	318	C–Cl in-plane bending	$69\beta_{C-Cl} + 19\beta_{CCC}$
a′	–	293 s	–	297 s	295	CCl_2 deformation	$51\delta_{CCl_2} + 20\beta_{CH} + 11\beta_{CC}$
a″	–	252 m	–	259 m	249	CCl_2 twisting	$60\tau_{CCl_2} + 21\omega_{CCl_2}$
a″	–	237 w	–	240 w	238	CCl_2 wagging	$51\omega_{CCl_2} + 28\tau_{CCl_2}$
a″	–	212 m	–	215 m	215	C–Cl out of plane bending	$44\gamma_{C-Cl} + 28\gamma_{CCC}$
a″	–	192 m	–	197 w	191	C–Cl out of plane bending	$56\gamma_{CCl_2} + 21\gamma_{CCC}$
a′	–	173 w	–	175 w	174	CCl_2 rocking	$68\pi_{CCl_2} + 21\delta_{CCl_2}$

[a] vs, very strong; s, strong; m, medium; w, weak; vw, very weak, ν, stretching; δ, deformation; β, in-plane bending; γ, out of plane bending; ρ, rocking; ω, wagging; τ, twisting/torsion.

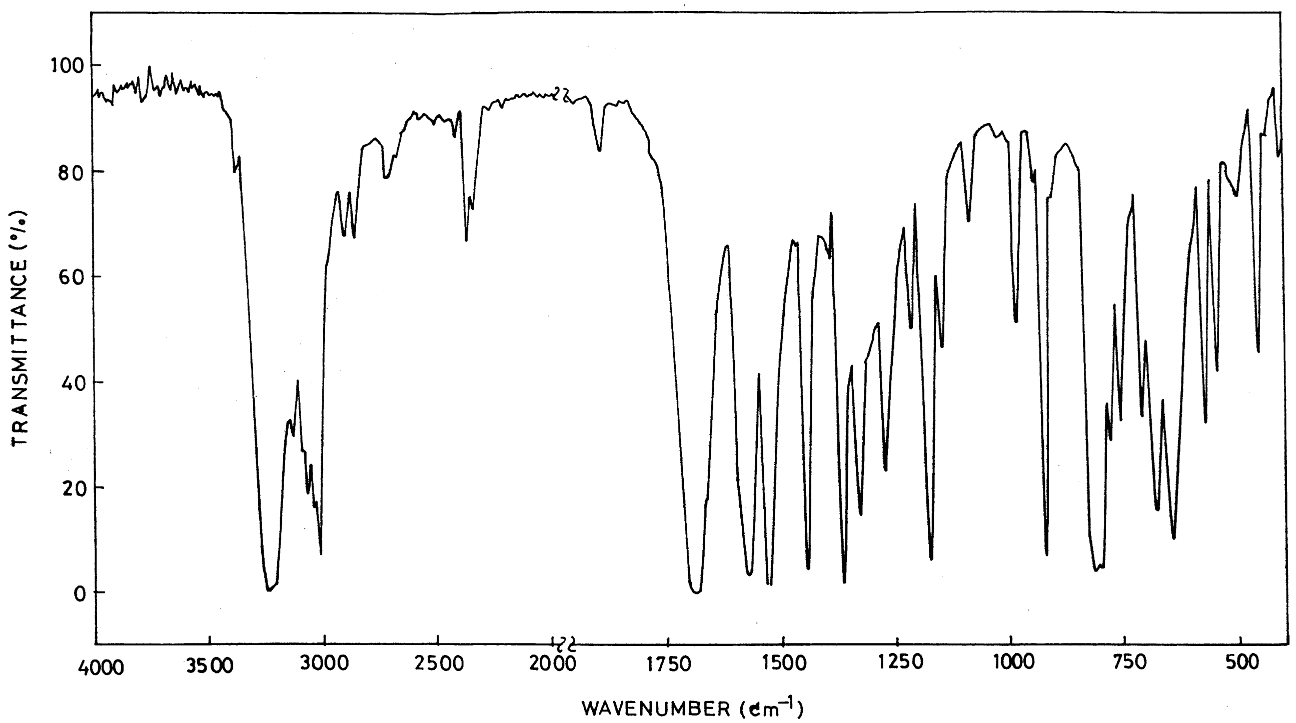

Fig. 12. FTIR spectrum of *N*-(2,3,4-trichlorophenyl)-2,2-dichloroacetamide.

and 3073, 3029 cm^{-1} are assigned to the C–H stretching modes in 246CPA.

4.4.1. Amide group vibrations

The amide group vibrational frequencies of 234CPA and 246CPA are found very close to each other and there is no difference in their magnitudes. The 234CPA and 246CPA shows very strong C=O absorption frequencies at 1688 and 1689 cm^{-1}, respectively, in the infrared. The corresponding Raman bands are seen at 1685 and 1687 cm^{-1}. The amide-I mode of the parent compound NPA is found at 1672 cm^{-1} in the infrared and 1680 cm^{-1} in Raman. The comparison clearly shows a slight increase in amide-I frequency of 234CPA and 246CPA. Similarly the other frequencies relating to amide-II, amide-III, amide-IV and amide-VI band does not show any appreciable variation when compared to

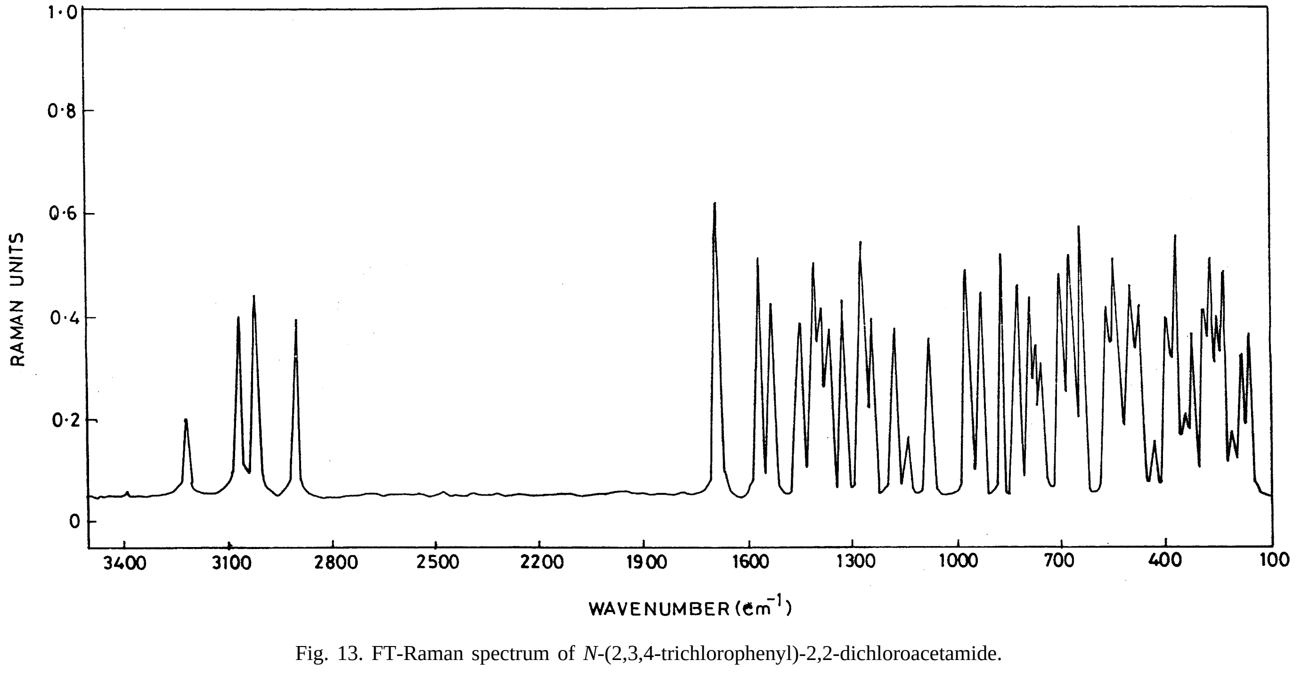

Fig. 13. FT-Raman spectrum of *N*-(2,3,4-trichlorophenyl)-2,2-dichloroacetamide.

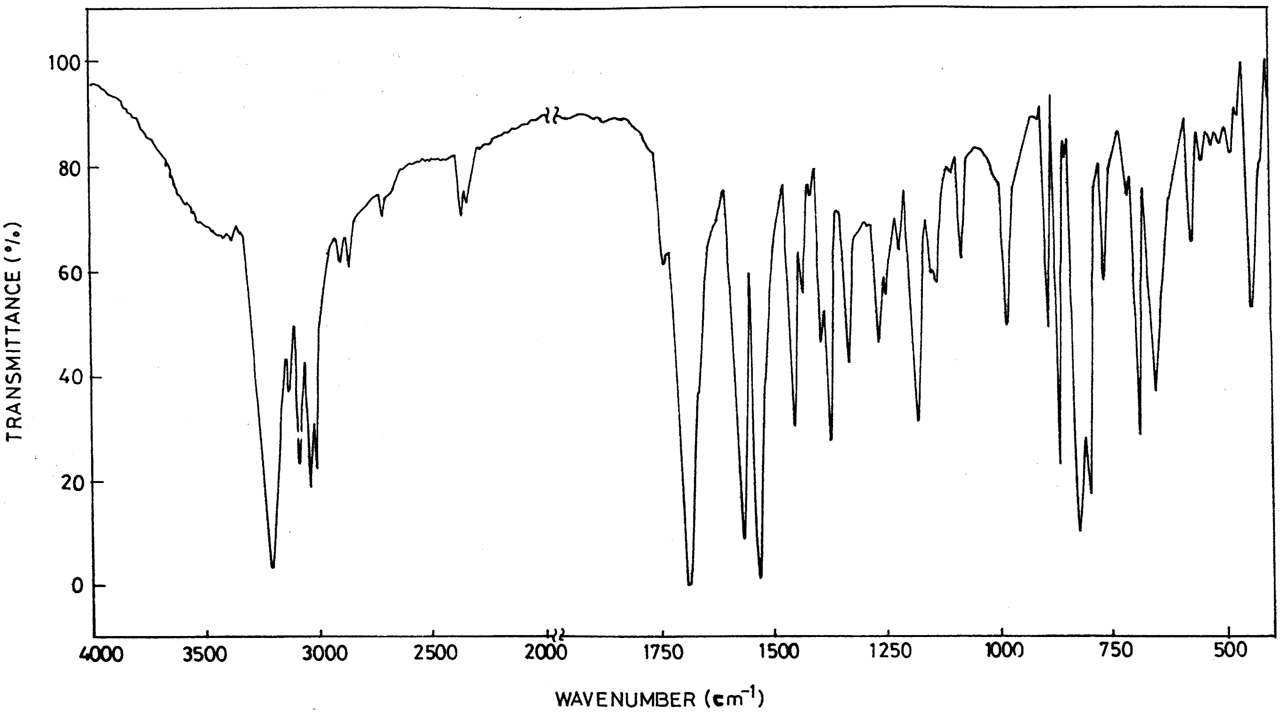

Fig. 14. FTIR spectrum of *N*-(2,4,6-trichlorophenyl)-2,2-dichloroacetamide.

NPA molecule and others. But the correlation of amide-V band of 234CPA and 246CPA with that of NPA clearly indicates that the frequencies are increased very significantly by about 40−50 cm^{-1} with that of NPA.

4.4.2. N–H stretching

The N–H stretching frequency of 234CPA is assigned to a very strong IR mode at 3219 cm^{-1} and the same is observed at 3211 cm^{-1} in 246CPA. The frequencies at 3217 cm^{-1} and 3219 cm^{-1} in Raman belongs to 234CPA and 246CPA, respectively. As explained earlier, the N–H stretching frequency is more influenced by the presence of intramolecular hydrogen bonding in *ortho*-chloro substituted compounds and found that the depression in magnitude of N–H stretching is more in the cases of 234CPA and 246CPA.

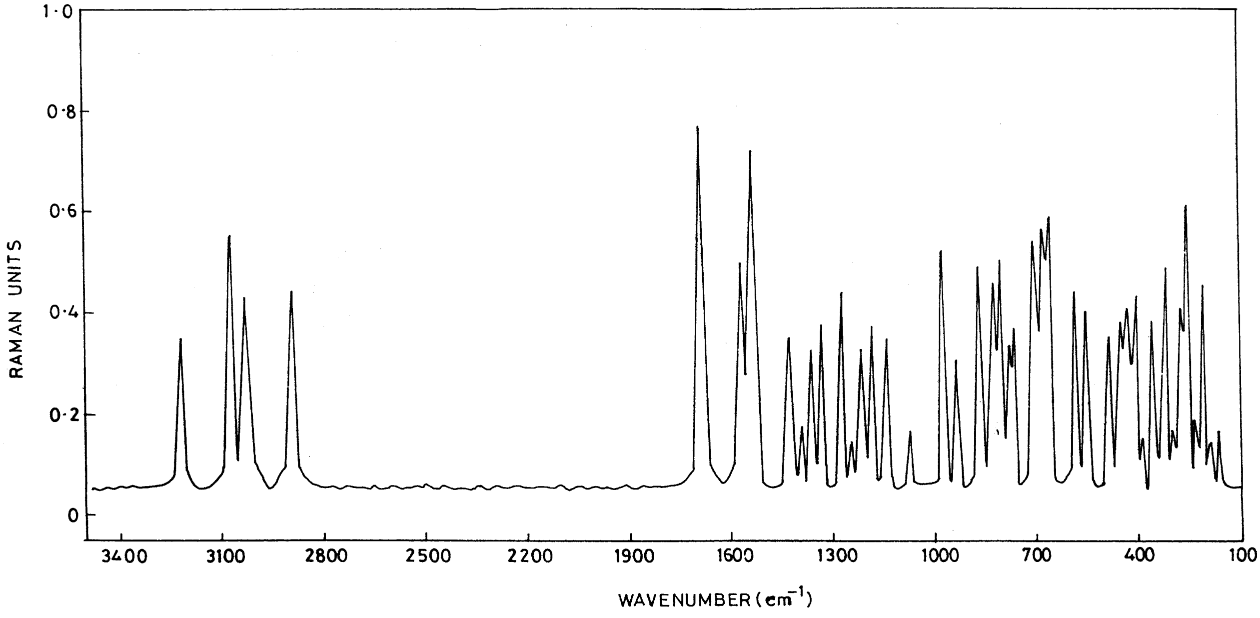

Fig. 15. FT-Raman spectrum of *N*-(2,4,6-trichlorophenyl)-2,2-dichloroacetamide.

Table 5
Observed and theoretical wavenumbers (cm^{-1}) and potential energy distribution (PED) for *N*-(2,3,4-trichlorophenyl)- and *N*-(2,4,6-trichlorophenyl)-2,2-dichloroacetamides[a]

Species	Observed wavenumber/int.				Calcluated wavenumber	Assignment	PED (%)
	N-(2,3,4-Trichlorophenyl)-2,2-dichloroacetamide		*N*-(2,4,6-Trichlorophenyl)-2,2-dichloroacetamide				
	FTIR	FTR	FTIR	FTR			
	3370 w	–	3374 vw	–		2 × 1688; 2 × 1689	
a'	3219 vs	3217 w	3211 vs	3219 m	3215	N–H stretching	$96\nu_{NH}$
	3134 s	–	3125 m	–		2 × 1573; 2 × 1568	
a'	3069 vs	3075 m	3077 s	3073 s	3075	C–H stretching	$91\nu_{CH}$
a'	3017 vs	3025 m	3030 s	3029 m	3028	C–H stretching	$94\nu_{CH}$
a'	2901 m	2905 m	2899 w	2903 m	2904	C–H(Cl$_2$) stretching	$81\nu_{CH} + 10\nu_{CC}$
	2857 m	–	2859 w	–		1573 + 1272; 1568 + 1264	
	2714 w	–	2707 vw	–		2 × 1371; 2 × 1374	
	2362 m	–	2359 vw	–		2 × 1177; 2 × 1179	
	2338 w	–	2338 vw	–		1688 + 643; 1689 + 652	
	1892 w	–	–	–		1330 + 573	
a'	1688 vs	1685 s	1689 vs	1687 vs	1681	C=O stretching	$71\nu_{C=O} + 20\nu_{CN}$
a'	1573 vs	1571 s	1568 vs	1569 s	1572	N–H in-plane bending	$71\beta_{NH} + 16\beta_{CN} + 10\beta_{CC}$
a'	1531 vs	1535 m	1532 vs	1535 vs	1531	C=C stretching	$86\nu_{CC}$
a'	1445 vs	1449 m	1453 s	–	1448	C=C stretching	$91\nu_{CC}$
a'	–	1429 s	1432 w	1430 m	1431	C=C stretching	$88\nu_{CC}$
a'	1393 vw	1389 m	1392 m	1398 w	1390	C–C stretching	$90\nu_{CC}$
a'	1371 vs	1368 m	1374 s	1368 m	1368	C–C stretching	$89\nu_{CC}$
a'	1330 vs	1328 m	1332 s	1331 m	1330	C–N stretching	$88\nu_{CN}$
a'						C–C stretching	$72\nu_{CC} + 11\nu_{CH} + 16\nu_{CN}$
a'	1272 s	1272 s	1264 m	1269 s	1252	N–C$_6$H$_5$ stretching	$52\nu_{NC} + 33\nu_{NH}$
a'					1270	C–C stretching	$78\nu_{CC} + 12\nu_{CH}$
a'	–	1248 m	1247 m	1245 w	1241	C–H(Cl$_2$) in-plane bending	$64\beta_{CH} + 24\beta_{C-Cl}$
a''	1216 m	–	1216 w	1220 m	1216	C–H(Cl$_2$) out of plane bending	$64\gamma_{CH} + 20\gamma_{CC}$
a'	1177 vs	1178 m	1179 s	1179 m	1171	C–H in-plane bending	$70\beta_{CH} + 18\beta_{CCC}$
a'	1148 m	1145 w	1140 m	1143 m	1142	C–H in-plane bending	$64\beta_{CH} + 28\beta_{CCC}$
a''	1087 w	1083 m	1078 m	1079 w	1080	C–H out of plane bending	$40\gamma_{CH} + 29\gamma_{CCC}$
a'	983 m	979 s	978 s	979 s	971	Trigonal bending	$94\beta_{CCC}$
a''	925 vs	929 s	–	932 m	930	C–H out of plane bending	$51\gamma_{CH} + 24\gamma_{CCC}$
a'	867 vw	869 s	864 vs	867 s	870	Ring breathing	$96\beta_{CCC}$
a'	–	827 s	824 vs	829 s	828	C=O in-plane bending	$76\beta_{C=O} + 18\beta_{CN}$
a'	799 vs	793 s	798 vs	796 s	791	CCl$_2$ asymmetric stretching	$69\nu_{C-Cl} + 19\nu_{CC} + 10\beta_{CH}$
a'	779 s	777 m	–	778 m	771	CCC in-plane bending	$61\beta_{CCC} + 21\beta_{CH}$
a''	755 s	759 m	761 m	759 m	749	N–H out of plane bending	$68\gamma_{NH} + 17\gamma_{CCC}$
a'					760	CCC in-plane bending	$49\beta_{CCC} + 21\beta_{CH} + 10\beta_{CN}$
a'	710 s	703 s	709 w	705 s	707	C–Cl stretching	$68\nu_{C-Cl} + 21\nu_{CC}$
a'	679 vs	673 s	–	674 s	676	C–Cl stretching	$71\nu_{C-Cl} + 19\beta_{CCC}$
a'	643 vs	645 s	652 s	650 s	648	CCl$_2$ symmetric stretching	$35\nu_{C-Cl} + 15\nu_{CC} + 10\nu_{CH}$
a'	573 s	575 m	571 m	575 m	571	C–Cl stretching	$74\nu_{C-Cl} + 15\beta_{CCC}$
a''	547 s	550 s	548 w	549 m	541	C=O out of plane bending	$39\gamma_{C=O} + 25\gamma_{CC} + 21\gamma_{CN}$
a'						C–C in-plane bending	$65\beta_{CC} + 28\beta_{CH}$
a'	500 w	505 m	507 vw	–	501	C–N in-plane bending	$55\beta_{CN} + 29\beta_{NH}$
a''	–	475 m	470 vw	476 m	471	C–N out of plane bending	$49\gamma_{CN} + 25\gamma_{C=O} + 19\gamma_{NH}$
a''						CCC out of plane bending	$35\gamma_{CCC} + 25\gamma_{C-Cl} + 24\gamma_{CH}$
a''	455 s	–	457 vw	452 m	455	CCC out of plane bending	$45\gamma_{CCC} + 25\gamma_{C-Cl} + 24\gamma_{CH}$
a'	438 vw	435 w	441 m	435 m	440	N–C$_6$H$_5$ in-plane bending	$40\beta_{NC} + 21\beta_{NH} + 20\beta_{CN}$
a''						C–C out of plane bending	$33\gamma_{CC} + 18\gamma_{CH} + 15\gamma_{CN}$
a''	405 w	407 m	–	399 m	398	N–C$_6$H$_5$ out of plane bending	$38\gamma_{NC} + 25\gamma_{NH} + 18\gamma_{CN}$
a'	–	375 s	–	377 w	371	C–Cl in-plane bending	$61\beta_{C-Cl} + 21\beta_{CCC}$
a'	–	351 w	–	350 m	346	C–Cl in-plane bending	$58\beta_{C-Cl} + 21\beta_{CCC}$
a'	–	329 m	–	331 s	321	C–Cl in-plane bending	$51\beta_{C-Cl} + 10\beta_{NH} + 12\beta_{CCC} + 14\beta_{CH}$
a'	–	301 m	–	303 w	302	CCl$_2$ deformation	$50\delta_{CCl_2} + 18\beta_{CH} + 17\beta_{CC}$
a''	–	275 s	–	277 m	264	CCl$_2$ twisting	$58\tau_{CCl_2} + 31\omega_{CCl_2}$
a''	–	247 m	–	250 s	242	CCl$_2$ wagging	$51\omega_{CCl_2} + 28\tau_{CCl_2}$
a''	–	229 s	–	225 w	221	C–Cl out of plane bending	$41\gamma_{C-Cl} + 29\gamma_{CCC} + 11\gamma_{CH}$
a''	–	205 w	–	200 m	201	C–Cl out of plane bending	$51\gamma_{C-Cl} + 24\gamma_{CCC}$
a''	–	190 m	–	185 w	181	C–Cl out of plane bending	$48\gamma_{C-Cl} + 14\gamma_{CN} + 10\gamma_{CCC} + 10\gamma_{CH}$
a'	–	169 m	–	168 w	171	CCl$_2$ rocking	$71\pi_{CCl_2} + 18\delta_{CCl_2} + 11\beta_{CN}$

[a] vs, very strong; s, strong; m, medium; w, weak; vw, very weak, ν, stretching; δ, deformation; β, in-plane bending; γ, out of plane bending; ρ, rocking; ω, wagging; τ, twisting/torsion.

Table 6
Correlation of amide (–CONH–) group vibrations of the compounds studied

Compound name	$\nu_{\mathrm{C=O}}$		$\beta_{\mathrm{N–H}}$		$\nu_{\mathrm{C–N}}$		$\beta_{\mathrm{C=O}}$		$\gamma_{\mathrm{N–H}}$		$\gamma_{\mathrm{C=O}}$		$\nu_{\mathrm{N–H}}$	
	FTIR	FTR	FTIR	FTR	FTIR	FTR	FTIR	FTR	FTIR	FTR	FTIR	FTR	FTIR	FTR
NPA	1672	1680	1555	1568	1344	1355	811	810	712	715	558	568	3270	3275
2CPA	1678	1685	1545	1551	1340	1346	807	804	739	742	574	–	3255	3253
4CPA	1676	1682	1555	1558	1338	1350	801	800	745	749	574	584	3277	3269
23CPA	1684	1680	1562	1567	1340	1345	809	816	740	749	573	571	3218	3215
24CPA	1682	1685	1569	1567	–	1342	812	815	–	752	570	567	3199	3201
234CPA	1688	1685	1573	1571	1330	1328	–	827	755	759	547	550	3219	3217
246CPA	1689	1687	1568	1569	1332	1331	824	829	761	759	548	549	3211	3219

4.4.3. Potential energy distribution

To check whether the chosen set of assignments contribute the most to the potential energy associated with normal co-ordinates of the molecules, the potential energy distribution has been calculated using the relation

$$\mathrm{PED} = \frac{F_{ii}L_{ik}^2}{\lambda_k}$$

where PED is the contribution of the ith symmetry co-ordinate to the potential energy of the vibrations whose frequency is ν_k, F_{ii} the force constant evaluated by the damped least square technique, L_{ik} the normalised amplitude of the associated element (i, k) and λ_k is the eigen value corresponding to the vibrational frequency k ($\lambda_k = 4\pi^2 c^2 \nu_k^2$). The PED contribution corresponding to each of the observed frequencies are listed in Table 6.

5. Conclusion

From the complete vibrational analysis of the FTIR and FT-Raman spectra of NPA, 2CPA, 4CPA, 23CPA, 24CPA, 234CPA and 246CPA molecules the following observations are made:

(i) Although the phenyl ring skeletal carbon–carbon stretching is insensitive to substitution, we found the substitution of chlorine atom in the ring diminished the carbon–carbon stretching frequencies particularly in the case of 234CPA and 246CPA but not much influenced in other compounds.

(ii) The comparison of amide group frequencies of the compounds under investigation shows that the presence of intramolecular hydrogen bonding between the chlorine atom and amide hydrogen specifically in the *ortho*-chloro substituted compounds like 2CPA, 23CPA, 24CPA, 234CPA and 246CPA. This is confirmed from the observed N–H stretching frequencies and found lowering in magnitudes of these vibrations in the case of *ortho*-chloro substituted compounds than that of NPA. The depressions in N–H stretching frequencies relative to NPA are not quantitative indications of the strength of intramolecular hydrogen bonding. The intramolecular hydrogen bonding is not favoured in the *para* chloro substituted molecule 4CPA.

(iii) The amide-I, C=O stretching frequency is slightly shifted to higher wavenumber in the cases of *N*-(chloro substituted phenyl) compounds than that of *N*-(phenyl)-2,2-dichloroacetamide (NPA). The magnitude of frequency variation is not significantly influenced by the position and number of chlorine atoms present.

(iv) The comparison of other amide group frequencies of the compounds did not show any appreciable variation in the respective wavenumbers. It has also been observed that the amide-V band, the N–H out of plane bending of *N*-(chloro substituted phenyl)-compounds is shifted to higher frequency than the *N*-(phenyl)-2,2-diclhoroacetamide.

(v) The FTIR and FT-Raman vibrational frequencies of the compounds under investigations revealed close similarities in the magnitudes of the frequencies of other similar modes in spite of the fact that the substituents in the phenyl ring are at different positions.

(vi) From the normal co-ordinate analysis we observed that most of the vibrations of the compounds investigated are remarkably pure modes with most of them composed of at least 70% of PED and above. Significant vibration interactions with other fundamentals are also observed, particularly in the low frequency region. The PED confirm the reliability and precision of the assignment and analysis of the vibrational fundamental modes.

References

[1] A.C. Scott, Physica D 51 (1990) 333.
[2] A.C. Scott, I.J. Bigio, C.T. Johnson, Phys. Rev. B 39 (1989) 12883.
[3] T. Benkui, P.P. John, Phys. Lett. A 240 (1998) 282.
[4] Y. Xiao, Phys. Lett. A 243 (1998) 174.
[5] J. Tekec, Z. Iric, Z. Przulj, J. Phys. Condens. Matter 10 (1998) 1487.
[6] O.F. Nielson, Asian J. Phys. 9 (2000) 139.
[7] D.M. Tessier, J. Marshall Clark, Anal. Chem. Acta 376 (1998) 103.
[8] R. Bartha, J. Agric. Food Chem. 16 (1968) 602.
[9] M.A. Alawi, Fresenius Anal. Chem. 312 (1982) 53.
[10] C.T. Johnson, S.F. Agnew, J. Eckert, L.H. Jones, B.I. Swanson, C.J. Unkefer, J. Chem. Phys. 95 (1991) 5281.
[11] J.L. Sauvajol, G. Denunzio, R. Almairac, J. Moret, M. Barthes, Solid State Commun. 77 (1991) 199.

[12] W.A. Herrebout, K. Clou, H.O. Desseyn, J. Phys. Chem. A 105 (2001) 4865.
[13] C.T. Johnson, B.I. Swanson, Chem. Phys. Lett. 114 (1985) 547.
[14] G. Careri, U. Buontempo, F. Galluzi, A.C. Scott, E. Gratton, E. Shyamsunder, Phys. Rev. B 30 (1984) 4689.
[15] J.L. Sauvajol, R. Almairac, J. Moret, M. Barthes, J.L. Ribet, J. Raman Spectrosc. 20 (1989) 517.
[16] K. Sree Ramulu, G. Ramana Rao, Indian J. Pure. Appl. Phys. 20 (1982) 372.
[17] E. Krishnamoorthy, G. Ramana Rao, J. Raman Spectrosc. 19 (1988) 359.
[18] E. Krishnamoorthy, G. Ramana Rao, J. Raman Spectrosc. 19 (1988) 419.
[19] E. Krishnamoorthy, G. Ramana Rao, J. Raman Spectrosc. 19 (1988) 439.
[20] E. Krishnamoorthy, G. Ramana Rao, J. Raman Spectrosc. 20 (1989) 409.
[21] K. Sree Ramulu, E. Krishnamoorthy, G. Ramana Rao, Indian J. Pure Appl. Phys. 21 (1983) 185.
[22] G. Ramana Rao, K. Venkata Ramiah, Indian J. Pure Appl. Phys. 18 (1980) 94.
[23] R. Sudarshan, G. Ramana Rao, V.V. Chalapathi, J. Raman Spectrosc. 21 (1990) 407.
[24] D. Krishna Bhat, B. Thimme Gowda, J. Indian Chem. Soc. 77 (2000) 279.
[25] S. Mathew, S. Ahmad, P.K. Verma, Spectrochim. Acta 50A (1994) 369.
[26] Y. Liu, M.A. Czavnecki, Y. Ozaki, Appl. Spectrosc. 48 (1994) 1095.
[27] R.A. Nyquist, D.A. Luoma, Appl. Spectrosc. 45 (1991) 1502.
[28] A. Spire, M. Barthes, H. Kelloui, G. De Nunzio, Physica D 137 (2000) 392.
[29] F.A. Berti, L.M. Ziti, Arch. Pharm. 285 (1952) 372.
[30] E.B. Wilson Jr., J. Chem. Phys. 7 (1939) 1047.
[31] E.B. Wilson Jr., J. Chem. Phys. 9 (1941) 76.
[32] E.B. Wilson, Jr., J.C. Decius, P.C. Cross, Molecular Vibrations, McGraw-Hill, New York, 1955.
[33] H. Fuhrer, V.B. Kartha, K.L. Kidd, P.J. Kruger, H.H. Mantsch, Computer Program for Infrared and Spectrometry, Normal Co-ordinate Analysis, vol. 5, National Research Council, Ottawa, Canada, 1976.
[34] L.E. Sutton, The Interatomic Bond Distances and Bond Angles in Molecules and Ions, London Chemical Society, London, 1958.
[35] D. Michalska, Spectrochim. Acta 49A (1993) 303.
[36] L.J. Bellamy, The Infrared Spectra of Complex Molecules, third ed., Wiley, New York, 1975.
[37] J.R. Durig, M.M. Bergana, H.V. Phan, J. Raman Spectrosc. 22 (1991) 141.
[38] L.K. Dyall, J.E. Kemp, Spectrochim. Acta 22 (1966) 483.
[39] G. Varsanyi, Assignments for Vibrational Spectra of Seven Hundred Benzene Derivatives, vol. I, Adam Hilger, London, 1974.